Topological and Geometric Methods with a View Towards Data Analysis

Der Fakultät für Mathematik und Informatik

der Universität Leipzig

eingereichte

DISSERTATION

zur Erlangung des akademischen Grades

DOCTOR RERUM NATURALIUM (Dr. rer. nat.)

im Fachgebiet Mathematik

vorgelegt von M.Sc.

Marzieh Eidi

geboren am 01.02.1989 in Tehran, Iran

Die Annahme der Dissertation wurde empfohlen von:

1. Professor Dr. Jürgen Jost(MPI MIS Leipzig)
2. Professor Norbert Peyerimhoff (Durham University, UK)

Die Verleihung des akademischen Grades erfolgt mit Bestehen der Verteidigung am 12.01.2022 mit dem Gesamtprädikat Magna Cum Laude.

Max-Planck-Institutfür Mathematik in then Naturwissenschaften

Leipzig

April 1, 2022

Acknowledgements

I am extremely grateful to all those people who helped me, who participated directly or indirectly in this work and supported me in the difficult times and specifically during my PhD studies which has been full of ups and downs; I hope they all feel some part of this work is theirs.

I sincerely thank my PhD supervisor Prof. Dr. Jürgen Jost for his heart-warming belief in my ability and for the doors that he has opened towards pure beauty in my view during our joyful discussions. I appreciate his availability, patience and encouragements which were always motivating me to go forward and not give up.

Many thanks to my lovely Iranian teachers and professors (in IPM institute and Sharif and Alzahra universities) for turning my interest in math to an unignorable love and in particular thanks to professor Mehrdad Shahshahi and professor Siavash Shahshahani who has been engraved in my mind as the hero of teaching forever and also for their great national legacy.

I would like to thank all those staff at Max Planck Institute for Mathematics in the sciences who supported me with their kind hospitality. I am grateful to my friends and colleagues in Iran and Germany who inspired me by their presence and hard work and for the happiness of unforgettable discussions; among all, I would like to name Dr Zahra Eidi, who is my sister, my dearest friend and a true inspiration for the scientific life and resistance.

I also thank the International Max-Planck Research School (IMPRS) for giving me the opportunity to pursue my studies in Leipzig.

Last but not least, my deepest appreciation goes to my beloved family for their unconditional love and endless support that made all this possible.

Dedication To

The sunlike presence of my mother

and

prosperous wishes of my father

Abstract

In geometry, various tools have been developed to explore the topology and other features of a manifold from its geometrical structure. Among the two most powerful ones are the analysis of the critical points of a function, or more generally, the closed orbits of a dynamical system defined on the manifold, and the evaluation of curvature inequalities. When any (nondegenerate) function has to have many critical points and with different indices, then the topology must be rich, and when certain curvature inequalities hold throughout the manifold, that constrains the topology. It has been observed that these principles also hold for metric spaces more general than Riemannian manifolds, and for instance also for graphs. This thesis represents a contribution to this program. We study the relation between the closed orbits of a dynamical system and the topology of a manifold or a simplicial complex via the approach of Floer. And we develop notions of Ricci curvature not only for graphs, but more generally for, possibly directed, hypergraphs, and we draw structural consequences from curvature inequalities. It includes methods that besides their theoretical importance can be used as powerful tools for data analysis. This thesis has two main parts; in the first part we have developed topological methods based on the dynamic of vector fields defined on smooth as well as discrete structures. To be more precise, we have introduced a Floer type boundary operator for generalised Morse-Smale dynamical systems on compact smooth manifolds which is defined based on counting the number of suitable flow lines between closed (both homoclinic and periodic) orbits and isolated critical points. We see that the same principle works for the discrete situation of general combinatorial vector fields, defined by Forman, on CW complexes and we show that we can recover the $\mathbb{Z}_2$ homology of both smooth and discrete structures directly from the flow lines (V-paths) of our vector field. In the second part, we concentrate on some curvature notions which already proved themselves as powerful measures for determining the local (and global) structures of smooth objects. Our main motivation here is developing methods which are helpful for the analysis complex networks. Many empirical networks incorporate higher order relations between elements and therefore are naturally modelled as, possibly directed and/or weighted, hypergraphs, rather than merely as graphs. In order to develop a systematic tool for the statistical analysis of such hypergraph, we propose a general definition of Ricci curvature on directed hypergraphs and explore the consequences of that definition. The definition generalizes Ollivier's definition for graphs. It involves a carefully designed optimal transport problem between sets of vertices. While

the definition looks somewhat complex, in the end we shall be able to express our curvature in a very simple formula, $\kappa = \mu_0 - \mu_2 - 2\mu_3$. This formula simply counts the fraction of vertices that have to be moved by distances 0, 2 or 3 in an optimal transport plan. We can then characterize various classes of hypergraphs by their curvature. In the last chapter, we show that our curvature notion is a powerful tool for determining complex local structures in variety of real and random networks modelled as (directed) hypergraphs. Furthermore, it can nicely detect hyperloop structures; hyperloops are fundamental in some real networks such as chemical reactions as catalysts in such reactions are faithfully modelled as vertices of directed hyperloops. Moreover with the help of Ollivier-Ricci curvature of reactions in the metabolic network of *Escherichia coli (E.coli)*, we can measure local clustering in these networks as the lowest amount of curvature corresponds to directed hypertrees and the highest amounts, which are very frequent, correspond to high clustering around a directed hyperedge. Also we see that the distribution of our curvature notion in real networks deviates from random models. In particular, by applying shuffling process on the wirings of this network, our notion can nicely detect the shuffling process while during this process degree sequence and size of hyperedges (both head and tail) remains stable.

Publications

Most of the ideas and figures of this thesis have appeared previously in the following publications:

1. Floer Homology: From Generalized Morse-Smale Dynamical Systems to Forman's Combinatorial Vector Fields, M.Eidi, J. Jost, arXiv, 2021.

2. Ollivier Ricci curvature of directed hypergraphs, M.Eidi, J. Jost, Nature Scientific Reports 2020, 10 (1).

3. Ricci curvature of random and empirical directed hypernetworks, W.Leal, M.Eidi, J.Jost, Applied network science 2020, 5 (1).

4. Edge-based analysis of networks: curvatures of graphs and hypergraphs, M.Eidi, A.Farzam, W.Leal, A.Samal, J.Jost, Theory in Biosciences 2020, 139 (4).

5. Curvature-based analysis of Directed Hypernetworks W.Leal, M.Eidi, J.Jost, The 8 th International Conference on Complex Networks and Their Applications 2019.
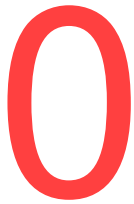
Contents

List of Figures

0 Motivations and Overview

Geometry is the science of measuring space, geo means earth and metry means measurement. There is a beautiful story behind the 2500 years development of this highly influential subject; classical geometry comes back to Euclid's work and studies shapes mostly in two dimensional and three dimensional Euclidean spaces. There, we study notions such as area, volume, length and angle and also the relations of these notions with each other. In classical geometry, all the geometrical properties of a shape will be preserved under (mirror) reflection, rotation or movement. In the 14th-century, philosopher and mathematician Nicole Oresme introduced the concept of curvature as a measure of departure from straightness. Then, the curvature of a differentiable curve was originally defined through osculating circles in the works of Cauchy; curvature was an infinitesimal quantity, obtained by taking second derivatives of functions describing shapes of smooth objects, like curves or surfaces. A fundamental step was taken by Gauss in the 19 century who defined the notion of intrinsic curvature of a surface. This curvature can be determined independently of the embedding into Euclidean (Flat) space, that is, by taking measurements only on that surface itself and not from any position outside that surface in space. Inspired by Gauss' discovery, Riemann proposed the concept of a "many fold extended quantity" which today is simply called a "manifold". A manifold is a geometric object which locally looks like Euclidean space of some dimension. Thus, a two-dimensional manifold is locally modelled by the Euclidean plane. In Riemannian geometry, curvatures obtained a deeper conceptual significance, as tensors encoding the geometric invariants of Riemannian metrics of smooth manifolds. In particular, the Ricci tensor is fundamental not only in Einstein's theory of general relativity and in elementary particle physics (the Calabi-Yau manifolds of string theory, for instance, are characterized by the vanishing of the Ricci tensor), but it also permeates much of modern research in Riemannian geometry.

Moreover due to the importance and deep insight that curvature notions have brought us in smooth settings, mathematicians in the past century have been interested in extending variety of curvature notions (specifically sectional and Ricci curvatures) to more general settings; they have been trying to develop notions such that:

- They are independent of infinitesimal properties such as continuity or differentiability and/or

- They have (some of) analytical/ geometrical or topological properties of curvature bounds in Riemannian manifolds.

- They can be applied to a wide range of examples and can be easily computed.

When we talk about Riemannian manifolds, all these manifolds are "locally" the same. But this resemblance is qualitative and not quantitative. Curvature is the fundamental geometric notion that helps us to quantitatively differentiate between different types of the manifolds in the same dimension. For studying the qualitative features of a manifold however we need to work with a more flexible type of geometry; Topology is the study of properties that are preserved not only under reflection, rotation or moving a shape but also under bending and stretching the shape. Geometrically, a circle and a square are two different shapes. In Topology we are looking for those properties that are not changed when we deform the shape continuously (namely we are not allowed to cut our shape). Some people consider Topology as the "fluid" Geometry; for instance, all the infinitely-many shapes that we can pass to obtain a circle from deforming a square (or vice versa) are topologically the same although they are different when seeing through the lens of classical Geometry. One of the properties that is preserved under topological changes is connectedness; if we deform our shape without cutting it, the number of its components would stay the same as before the deformation. More generally, the same happens if we consider the number of k-dimensional holes of our n-dimensional manifold (for $0 \leq k \leq n$) as their numbers are fixed no matter how we deform our shape as long as the deformation is continuous. If we consider the example of circle and square again, both of them have one connected component and a 1-dimensional hole. Similarly, sphere and cube are both connected spaces which have no 1-dimensional hole but both of them encircle a two-dimensional hole. Although intuitively we can tell the number of these parameters easily for simple shapes, for more complicated ones, finding the number of holes in arbitrary dimensions has been a challenging problem and a variety of beautiful theories have been introduced in the past century to tackle this problem. Algebraic Topology is the branch of mathematics where we study invariance of such properties under topological transformations in terms of algebraic notions and in particular Homology theory is concerned about the number of holes. There we assign a sequence of algebraic structures to each object to get the number of its holes in all dimensions.

Nowadays, one of our main challenges is to understand the shape of "Big Data"; the total amount of data created, captured, copied, and consumed globally is reaching 79 zettabytes in 2021 and is forecast to increase rapidly to more than 180 zettabytes in 2025 [28]. This is even more than what was expected before, due to the COVID-19 pandemic, since more work and education has been done online. Scientists are confronted with a very massive amount of data and apart from the issue of finding more storage capacity, our main problem is to

recognise which part of data is essential to be stored, which part is noisy or redundant, how we can get useful information from this highly complex data and what are those features of data that can give deep insight to its structure.

In modern data analysis, we use topological and geometric methods to investigate its shape and fundamental properties. With the help of Geometry we can analysis local structures, uncover the main patterns and find the most important parts of data; on the other side, Topology, as opposed to Geometry, does not need to measure distances, thus is a very powerful and natural tool to find the persistent features and non-noisy data that form its global shape. As data is usually discrete and presented by finite number of points, we need to utilize and/or develop mathematical notions that can be applied to discrete structures such as real networks, that are modelled as graphs, hypergraphs and simplicial complexes (and more generally polyhedral complexes). Sometimes we also consider the smooth shapes and then with the help of these discrete notions we approximate our smooth shape with a sequence of the discrete ones.

Besides the very important application for discrete data analysis, development of such discrete or more general tools in return has put further fascinating theoretical problems in front of us. On the other side, in smooth settings, Geometry and Topology have deep connections as when certain curvature inequalities hold throughout the manifold, that constrains the topology; thus a main question is how much such connections can be transferred to more general or discrete settings.

Topological and Geometric Data Analysis are rapidly growing fields that have profoundly empowered our techniques for visualising, simulating and analysing data. Topological data analysis gives us insight to both continuous and discrete properties of data and have found many applications in different domains ranging from neuroscience to cancer biology, road networks and even astronomy.

The demand of more powerful and faster methods has motivated us to develop a type of Homology theory, called Floer homology in this thesis that can help us to determine the structure of both smooth and discrete shapes with the help of geometric notions such as vector fields.

On the other side, Geometric data analysis is a very useful approach for variety of purposes such as dimensionality reduction of data sets, which are represented by high dimensional vectors (Matrices and Tensors), as well as probing the local patterns of huge and complex structures. In the second part of these thesis, we try to develop our geometric perspective for looking at data; more precisely, we develop some discrete curvature notions that can be considered as powerful tools for the analysis of complex networks such as chemical reactions.

The interaction between Topology, Geometry and Data Science have brought us many beautiful opportunities; Topological and Geometric Data Analysis are relatively new topics and rapidly penetrating different aspects of Data Science as they have been formed based on

theoretical advances reached over the centuries. In this thesis we aim at bringing together some of our recent developed results on geometrical and topological methods on smooth as well as discrete structures and at the end we briefly show the power and advantage of some of these methods for analysing real data sets.

Organization of the thesis:

Chapter zero at the beginning, gives an overview of topological and geometric methods presented in this thesis ; afterwards, this thesis consists of two main parts and each part includes three chapters; the first chapter of each part is an introduction for the other two chapters. The first part is on topology and dynamics of smooth and discrete structures; the second part concerns about some geometric methods and in particular discrete curvature notions and their application in the analysis of complex networks. In chapter two, we firstly define the basic concepts about Morse-Smale dynamical systems on smooth closed manifolds and we then propose our Floer type boundary operator for these systems and at the end of the chapter we present some concrete examples of how to compute homology groups with the help of our operator. In chapter three, we focus on dynamical systems on combinatorial settings and in particular CW complexes. We extend the idea of Morse-Floer-Forman boundary operator to the general combinatorial vector fields which was originally defined by Forman. At the end of chapter three, we propose some examples of computing homology groups for these structures. After the introductory chapter four for the second part, chapter five is about the concept of discrete curvature notions and in particular Ollivier-Ricci curvature which was defied originally by Ollivier for Markov chains on metric measure spaces. We extend this notion to the more general and complex structure of directed hypergraphs and we show how we can characterise hypergraphs with the help of their curvatures. in the final chapter, chapter 6, we apply curvature notions to random and real networks; we focus on chemical reaction networks and in particular metabolic network of a bacteria, *Escherichia coli (E.coli)*, and we show why our curvature notions can be used as powerful tools for the analysis of complex networks.

Part I

Topology and Dynamic

1 Introduction

One of the key ideas of modern geometry is to extract topological information about an object from a dynamical process operating on that object. For that purpose, one needs to identify the invariant sets and the dynamical relations between them. The invariant sets generate groups, and the dynamics defines boundary operators, and when one has shown that these operators square to zero, one can then define homology groups. The first such ideas may be seen in the works of Riemann, Cayley and Maxwell in the 19th century. In 1925, Morse [43] developed his famous theory where he recovered the homology of a compact Riemannian manifold M from the critical points of a smooth function f, assuming that these critical points are all non-degenerate. The dynamics in question is that of the gradient flow of f. The basic invariant sets then are precisely the critical points of f. The theory was analyzed and extended by Milnor, Thom, Smale, Bott and others. In particular, Bott [7] extended the theory to the case where the gradient of f is allowed to vanish on a collection of smooth submanifolds of M.

Based on ideas from supersymmetry, Witten constructed an interpolation between de Rham and Morse homology. Floer [20] then developed the very beautiful idea that the boundary operator in Morse theory can be simply obtained from counting gradient flow lines (with appropriate orientations) between critical points of index difference one. The first systematic exposition of Floer's ideas was given in [52] (see also [32]). The main thrust of Floer's work was devoted to infinite dimensional problems around the Arnold conjecture, see [17–19, 22], because for his theory, he only needed relative indices, and not absolute ones, so that the theory could be applied to indefinite action functionals. But also in the original finite dimensional case, Floer's theory advanced our insight considerably and motivated much subsequent work.

In fact, Floer [20] had been motivated by another beautiful theory relating dynamics and topology, that of Conley [9] (for more details, see [10] and for instance the presentations in [31, 56]). Conley's theory applies to arbitrary dynamical systems, not just gradient flows. Actually, Smale [54] had already extended Morse theory to an important and general class of dynamical systems on compact Riemannian manifolds, those that besides isolated critical points are also allowed to have non-degenerate closed orbits. Similar to Morse functions,

the class of Morse-Smale dynamical systems is structurally stable, that is, preserves its qualitative properties under small perturbations. It turns out, however, that these systems can also be subsumed under Morse-Bott theory. In fact, in [55] Smale proved that for every gradient-like system there exists an energy function that is decreasing along the trajectories of the flow, and Meyer [42] generalized this result to the Morse-Smale dynamical systems and defined a Morse-Bott type energy function based on the flows. Such an energy function would then be constant on the periodic orbits, and they can then be treated as critical submanifolds via Morse-Bott theory. Banyaga and Hurtubise [3, 4, 29] then constructed a general boundary operator for Morse-Bott systems that put much of the preceding into perspective (see also the detailed literature review in [29]).

There is still another important extension of Morse theory, the combinatorial Morse theory of Forman [25] on simplicial and cell complexes. Here, a function assigns a value to every simplex or cell, and certain inequalities between the values on a simplex and on its facets are required that can be seen as analogues of the non-degeneracy conditions of Morse theory in the smooth setting. As shown in [6], this theory recovers classical Morse theory by considering PL triangulations of manifolds that admit Morse functions. This theory has found various practical applications in diverse fields, such as computer graphics, networks and sensor networks analysis, homology computation, astrophysics, neuroscience, denoising, mesh compression, and topological data analysis. (For more details on smooth and discrete Morse theory and their applications see [34, 53]). In [23], Forman also extended his theory to combinatorial vector fields.

In the first chapter of this part, we extend Floer's theory into the direction of Conley's theory. More precisely, we shall show that one can define a boundary operator by counting suitable flow lines not only for Morse functions, but also for Morse-Smale dynamical systems, and in fact, we more generally also allow for certain types of homoclinic orbits in the dynamical system. Perhaps apart from this latter small extension, our results in the smooth setting readily follow from the existing literature. One may invoke [42] to treat it as a Morse-Bott function with the methods of [29]. Alternatively, one may locally perturb the periodic orbits into heteroclinic ones between two fixed points by a result of Franks [27] and then use [55] to treat it like a Morse function. In some sense, we are also using such a perturbation. Our observation then is that the collection of gradient flow lines between the resulting critical points has a special structure which in the end will allow us to directly read off the boundary operator from the closed (or homoclinic) orbits and the critical points. It remains to develop Conley theory in more generality from this perspective. Moreover, our approach also readily extends to the combinatorial situation of [23, 25]. Again, it is known how to construct a Floer type boundary operator for a combinatorial Morse function, and an analogue of Witten's approach had already been developed in [24]. Our construction here, however, is different from that of that paper. In fact, [24] requires stronger assumptions on the function than the Morse condition, whereas our construction needs no further assumptions.

What we want to advocate foremost, however, is that the beauty of Floer's idea of counting flow lines to define a boundary operator extends also to dynamical systems with periodic orbits, in both the smooth and the combinatorial setting, and that a unifying perspective can be developed.

We should point out that in this part and for both of the next chapters, we only treat homology with $\mathbb{Z}_2$ coefficients. Thus, we avoid having to treat the issue of orientations of flow lines. This is, however, a well established part of the theory, see [21] or also the presentations in [32, 52]. These chapters are based on our preprint, Floer Homology: From Generalized Morse-Smale Dynamical Systems to Forman's Combinatorial Vector Fields [14].

2

Floer Homology of Generalised Morse-Smale Dynamical Systems

This chapter is about the extension of smooth theories of Morse and Floer. In Morse-Floer theory, we can compute Betti numbers of a closed manifold with the help of a boundary operator associated to the negative gradient flow lines of a Morse function. Recall that a Morse function, is a real valued function on a closed manifold that all its critical points are nondegenerate, that is, the Hessian of the function is nondegenerate at every critical point. While in Morse theory the critical points have to be isolated and in Floer's beautiful idea we consider the gradient flow lines between these points, in this chapter we extend the scope of Morse-Floer theory to a dynamical system that is allowed to have finite number of closed orbits. The systems that we consider is a slight generalisation of Morse-Smale dynamical systems as we are allowed to have finite number of homoclinic points and orbits as well as periodic orbits. What we need to consider is not only the flow lines between the critical points but also the flow lines between critical points as well as closed orbits

<h2>2.1 Preliminaries</h2>

We consider a smooth m dimensional manifold M that is closed, oriented and equipped with a Riemannian metric whose distance function we denote by d. Let X be a smooth vector field on M and $\phi_t : M \longrightarrow M$ be the flow associated to X. We first recall some basic terminology. For $p \in M$, $\gamma(p) = \cup_t \phi_t(p)$ will denote the trajectory of X through p. Then for each $p \in M$ we define the limit sets of $\gamma(p)$ as

$$\begin{aligned} \alpha(p) &:= \cap_{s \leq 0} \overline{\cup_{t \leq s} \phi_t(p)} \\ \omega(p) &:= \cap_{s \geq 0} \overline{\cup_{t \geq s} \phi_t(p)}. \end{aligned}$$

Definition 2.1.1. *If $f : M \to M$ is a diffeomorphism, then $x \in M$ is called* chain recurrent *if for any $\varepsilon > 0$ there exist points $x_1 = x, x_2, ..., x_n = x$ (n depends on ε) such that $d(f(x_i), x_{i+1}) < \varepsilon$ for $1 \leq i \leq n$. For a flow ϕ_t, $x \in M$ is* chain recurrent *if for any $\varepsilon > 0$ there exist points $x_1 = x, x_2, ..., x_n = x$ and real numbers $t(i) \geq 1$ such that $d(\phi_{t(i)}(x_i), x_{i+1}) < \varepsilon$ for $1 \leq i \leq n$. The set of chain recurrent points is called the* chain

recurrent set *and will be denoted by $R(X)$.*

The *chain recurrent set* $R(X)$ is a closed submanifold of M that is invariant under ϕ_t. We can think of $R(X)$ as the points which come within ε of being periodic for every $\epsilon > 0$. A Morse-Smale dynamical system, as introduced by Smale [54], has the fundamental property that it does not have any complicated recurrent behaviour and the α and ω limit sets of every trajectory can only be rest points p or periodic orbits O. Morse-Smale dynamical systems are the simplest structurally stable types of dynamics; that is if X is Morse-Smale and X' is a sufficiently small C^1 perturbation of X then there is a homeomorphism $h : M \rightarrow M$ carrying orbits of X to orbits of X' and preserving their orientation (Such a homeomorphism is called topological conjugacy and we say that the two vector fields or their corresponding flows are topologically conjugate). Here, we shall consider a somewhat more general case where we allow for a certain type of homoclinic rest points and their homoclinic orbits.

Definition 2.1.2. *A periodic orbit of the flow ϕ_t on M is hyperbolic if the tangent bundle of M restricted to O, $TM \mid_O$, is the sum of three derivative $D\phi_t$ invariant bundles $E^c \oplus E^u \oplus E^s$ such that:*

1. *E^c is spanned by the vector field X, tangent to the flow.*

2. *There are constants $C, \lambda > 0$, such that $\parallel D\phi_t(v) \parallel \geqslant Ce^{\lambda t} \parallel v \parallel$ for $v \in E^u, t \geqslant 0$ and $\parallel D\phi_t(v) \parallel \leqslant C^{-1}e^{-\lambda t} \parallel v \parallel$ for $v \in E^s, t \geqslant 0$ where $\parallel \parallel$ is some Riemannian metric.*

A rest point (also called critical) p for a flow ϕ_t is called hyperbolic provided that $T_pM = E^u \oplus E^s$ and the above conditions are valid for $v \in E^u$ or E^s.

The stable and unstable manifolds of a hyperbolic periodic orbit O, are defined by: $W^s(O) = \{x \in M \mid d(\phi_t x, \phi_t y) \rightarrow 0$ as $t \rightarrow \infty$ for some $y \in O\}$ and $W^u(O) = \{x \in M \mid d(\phi_t x, \phi_t y) \rightarrow 0$ as $t \rightarrow -\infty$ for some $y \in O\}$. For an isolated rest point and a homoclinic orbit, we define the stable and unstable manifolds analogously. Also the index of an isolated rest point or a closed orbit is defined to be the dimension of E^u.

We denote an arbitrary point in a homoclinic orbit H by H_k^0 where k is the index of the homoclinic orbit H and the homoclinic orbit itself is denoted by H_k^1 as it is homeomorphic to a circle and therefore is one-dimensional. Similarly by O_k^0 we mean an arbitrary point in a periodic orbit O of index k and by O_k^1 we mean the orbit itself as a one dimensional structure, homeomorphic to a circle.

In the following definition we extend the definition of Morse-Smale vector fields.

Definition 2.1.3. *We call a smooth flow ϕ_t on M generalised Morse-Smale if :*

1. *The chain Recurrent set of the flow consists of a finite number of (isolated) hyperbolic rest points $\beta_1(p),... \beta_k(p)$ and hyperbolic periodic orbit $\beta_{k+1}(O),... \beta_n(O)$.*

2. $R(X)$ *furthermore has a finite number of homoclinic orbits $\beta_{n+1}(H),... \beta_l(H)$ that can be obtained via local bifurcation from hyperbolic periodic orbits $\beta_{n+1}(O), ..., \beta_l(O)$.*

3. *For each $\beta_i(p), 1 \leq i \leq k$ and each $\beta_i(O), k+1 \leq i \leq l$ the stable and unstable manifolds $W^s(\beta_i)$ and $W^u(\beta_i)$ associated with β_i intersect transversally.*
   (Here, two such submanifolds intersect transversally if for every $x \in W^u(\beta_i) \cap W^s(\beta_j)$ we have: $T_x(M) = T_x W^u(\beta_i) \bigoplus T_x W^s(\beta_j)$.)

Note that the only difference between generalised Morse-Smale flows as defined here and standard Morse-Smale flows is the possible existence of homoclinic points and orbits. In the standard case, one simply excludes the second condition.

Therefore a generalised Morse-Smale flow can be perturbed to a corresponding Morse-Smale flow where all of the homoclinic orbits $\beta_i(H), n+1 \leq i \leq l$ are substituted by periodic orbits $\beta_i(O)$. For any two distinct β_i and β_j in the above definition we consider $W(\beta_i, \beta_j) = W^u(\beta_i) \cap W^s(\beta_j)$. Then based on the transversality condition, this intersection is either empty (if there is no flow line from β_i to β_j or a submanifod of dimension $\lambda_{\beta_i} - \lambda_{\beta_j} + \dim \beta_i$ where the index of β_k is denoted by λ_{β_k} [4]. For any two critical B and B' the flow ϕ_t induces an $\mathbb{R}$-action on $W(B, B') = W^u(B) \cap W^s(B')$. Let

$$M(B, B') = (W(B, B'))/\mathbb{R}$$

be the quotient space by this action of the flow lines from B to B'.

Remark 2.1.4. *In the definition of standard Morse-Smale flow the (1) above could be replaced by $(1')$:*
All periodic orbits and rest points of the flow are hyperbolic and there exists a Morse-Bott type energy function (as Meyer defined [42]).

2.2 The chain complex for generalized Morse-Smale vector fields

Suppose X is a generalized Morse-Smale vector field over M. To motivate our construction, we first observe that by a slight extension of a result of Franks [27], we can replace every periodic or homoclinic orbit by two non-degenerate critical points, without changing the flow outside some small neighbourhood of that orbit.

Lemma 2.2.1. *Suppose ϕ_t is a generalized Morse-Smale flow on an orientable manifold with a periodic or homoclinic orbit of index k. Then for any neighbourhood U of that orbit there exists a new generalized Morse-Smale flow ϕ'_t whose vector field agrees with that of ϕ_t outside U and which has rest points t and t' of index $k+1$ and k in U but no other chain recurrent points in U.*
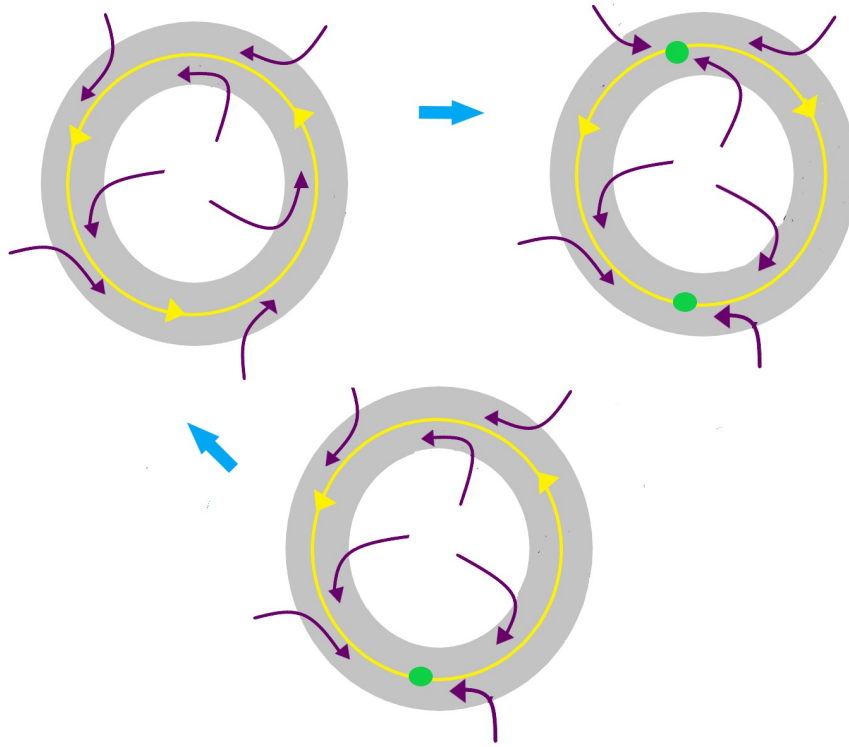
Proof. In [27] Franks proved that for a Morse-Smale flow ϕ_t on an orientable manifold with a closed periodic orbit O of index k and a given neighbourhood U of O, there exists a new Morse-Smale flow ϕ'_t whose vector field agrees with that of ϕ_t outside U and which has rest points q_1 and q_2 of index k and $k+1$ in U but no other chain recurrent points in U.

For the generalized Morse- Smale flow we note that each homoclinic orbit is by definition obtained in a continuous local bifurcation of a periodic orbit. Therefore if we use this bifurcation in the reverse direction and substitute again any such homoclinic orbit with its corresponding periodic orbit we can use Franks' argument for replacing all the periodic and homoclinic orbits with two rest points and two heteroclinic orbits between them. $\square$

Remark 2.2.2. *In the above figure, the qualitative feature of the three cases outside the gray annulus are the same; In particular, we can bifurcate two heteroclinic orbits between two critical points (in the right) to get a hmoclinic orbit and homoclinic critical point (in the middle) by making the two critical points closer and closer and then bifurcate the homoclinic orbit to a periodic orbit (in the left).*

With this lemma, we can turn our flow into one that has only non-degenerate critical points. We could then simply utilize the Floer boundary operator for that flow. In fact, that motivates our construction, but we wish to define a Floer type boundary operator directly in terms of the periodic and homoclinic orbits and the critical points. Our simple observation is that a Floer boundary operator resulting from the replacement that Franks proposed, has

some additional structure that is derived from the orbits that have been perturbed away. This allows for an arrangement of the flow lines between the critical points of the perturbed flow that leads to the definition of the boundary operator in the presence of those orbits. That is, we can read off the boundary operator directly from the relations between the orbits and the critical points without appealing to that perturbation, although the perturbation helps us to see why this boundary operator squares to 0. We define the Morse-Floer complex $(C_*(X), \partial)$ of X as follows. Let C_k denote the finite vector space (with coefficients in $\mathbb{Z}_2$) generated by the following set of rest points/orbits of the vector field :

$$\left(p_k, O_k^0, O_{k-1}^1, H_k^0, H_{k-1}^1\right).$$

The differential $\partial_k : C_k(X) \longrightarrow C_{k-1}(X)$ counts the number of connected components of $M(\beta_i, \beta_j)$ (mod 2) where β_i and β_j are isolated rest points p_k or closed orbits (either homoclinic orbits H or periodic orbits O). Here, each such orbit, carrying topology in two adjacent dimensions, corresponds to two elements in the boundary calculus. More precisely, a periodic orbit O_k of index k generates an element O_k^1 in dimension $k + 1$ and an element O_k^0 in dimension k, and analogously for the homoclinics. Thus, our boundary operator is

$$\partial p_k = \sum \alpha(p_k, p_{k-1})p_{k-1} + \sum \alpha(p_k, O_{k-2})O_{k-2}^1$$
$$+ \sum \alpha(p_k, H_{k-2})H_{k-2}^1$$

$$\partial O_{k-1}^1 = \sum \alpha(O_{k-1}, O_{k-2})O_{k-2}^1 + \sum \alpha(O_{k-1}, H_{k-2})H_{k-2}^1$$

$$\partial O_k^0 = \sum \alpha(O_k, O_{k-1})O_{k-1}^0 + \sum \alpha(O_k, H_{k-1})H_{k-1}^0$$
$$+ \sum \alpha(O_k, p_{k-1})p_{k-1}$$

$$\partial H_{k-1}^1 = \sum \alpha(H_{k-1}, H_{k-2})H_{k-2}^1 + \sum \alpha(H_{k-1}, O_{k-2})O_{k-2}^1$$

$$\partial H_k^0 = \sum \alpha(H_k, H_{k-1})H_{k-1}^0 + \sum \alpha(H_k, O_{k-1})O_{k-1}^0$$
$$+ \sum \alpha(H_k, p_{k-1})p_{k-1}.$$

In this definition, the sums extend over all the elements on the right hand side; for instance, the first sum in the first line is over all critical points p_{k-1} of index $k - 1$. $\alpha(p_k, p_{k-1})$, similar to the classical Morse-Floer theory (where there is no closed orbit and therefore the vector field is gradient-like), is the number of flow lines from p_k to p_{k-1}. We observe some terms do not appear; for instance, we do not have terms with coefficients of the form $\alpha(p_k, O_{k-1}^0)$. This will be important below in the proof of Thm. 2.2.4. The reason why such a term does not show up is that if there were a flow line from some p_k to some O_{k-1}^0, then there would

also be a flow to the corresponding O_{k-1}^1 which comes from the same closed orbit. But O_{k-1}^1 and p_k are the elements of the same C_k, and by the Morse-Smale condition, there are no flow lines between critical elements of the same C_k. Analogously for homoclinics.

Remark 2.2.3. *Note that in defining the chain complex and the corresponding boundary operator ∂ for X, we could first replace all the homoclinic orbits with bifurcated periodic orbits and present our definitions for the simpler case where all the closed orbits are periodic. Then we would have just three generators*

$$\left(p_k, O_k^0, O_{k-1}^1\right)$$

for $C_k(X)$. However here we choose not to do this to emphasize that we can construct the boundary operator also for homoclinic orbits as long as our operator is defined based on the flow lines outside the tubular neighbourhoods of orbits.

Theorem 2.2.4. $\partial^2 = 0$.

In classical Morse-Floer theory, one assumes that there are only isolated critical points and no closed or homoclinic orbits, and therefore all the α coefficients in the definition of ∂ except the first one (in the first row) are zero; there to prove $\partial^2 = 0$ one can then use the classification theorem of one dimensional compact manifolds where the number of connected components of their boundary mod two is zero (see [32]). Here as $W(\beta_i, \beta_{i-1})$ might have dimension bigger than one, the number of connected components of the boundary of compact two dimensional manifolds might vary. For our generalized Morse-Smale flows, however, we use Lemma 2.2.1 to replace any orbit of index k (both periodic O_k and homoclinic H_k) by a rest point of index k and one of $k+1$ which are joined by two heteroclinic orbits. When replacing H_k, the resulting rest point of higher index can be taken to be the point h itself, which then will be no longer homoclinic.

Proof. By the above replacement, we get a vector field Y which has no periodic and homoclinic orbits and is therefore gradient-like (up to topological conjugacy). This Y has all the isolated rest points of X, two isolated rest points q_k^{up} and $q_{k-1}^{\prime down}$ instead of every periodic orbit O_{k-1} of index $k-1$ and two isolated rest points t_k^{up} and $t_{k-1}^{\prime down}$ instead of every homoclinic orbit H_{k-1} of index $k-1$. We note that all the critical points in Y are isolated and for each index k they can be partitioned into five different sets $p_k, t_k^{up}, t_k^{\prime down}, q_k^{up}, q_k^{\prime down}$. This partitioning is possible because orbits and isolated rest points have pairwise empty intersection. The proof will now consist of the following main steps:

1. We define $C_k(Y)$ to be the finite vector space (with coefficients in $\mathbb{Z}_2$) generated by

$$\left(p_k, q_k^{up}, q_k^{\prime down}, t_k^{up}, t_k^{\prime down}\right)$$

.

2. We define a boundary operator ∂' and consequently a chain complex corresponding to $(Y, C_*(Y), \partial')$.

3. and then we prove there is an isomorphism (chain map) $\varphi_* : C_*(X) \longrightarrow C_*(Y)$. Since φ is an isomorphism we get our desired equality $\partial^2 = 0$ as $\partial = \varphi_*^{-1} \partial' \varphi_*$ and $\partial^2 = \varphi_*^{-1} \partial'^2 \varphi_*$

   1. We note that in $C_k(Y)$, q_k^{up} comes from a periodic orbit of index $k - 1$ and $q_k'^{down}$ comes from the replacement of a periodic orbit of index k. Similarly t_k^{up} is obtained from replacing a homoclinic orbit of index $k - 1$ and $t_k'^{down}$ comes from a homoclinic orbit of index k.

   2. We define $\partial_k' : C_k(Y) \longrightarrow C_{k-1}(Y)$ as follows:

$$
\begin{aligned}
\partial' p_k &= \sum \alpha(p_k, p_{k-1})p_{k-1} + \sum \alpha(p_k, q_{k-1}^{up})q_{k-1}^{up} \\
&+ \sum \alpha(p_k, t_{k-1}^{up})t_{k-1}^{up}
\end{aligned}
$$

$$
\begin{aligned}
\partial' q_k^{up} &= \sum \alpha(q_k^{up}, q_{k-1}^{up})q_{k-1}^{up} \\
&+ \sum \alpha(q_k^{up}, t_{k-1}^{up})t_{k-1}^{up}
\end{aligned}
$$

$$
\begin{aligned}
\partial' q_k'^{down} &= \sum \alpha(q_k'^{down}, q_{k-1}'^{down})q_{k-1}'^{down} \\
&+ \sum \alpha(q_k'^{down}, t_{k-1}'^{down})t_{k-1}'^{down} \\
&+ \sum \alpha(q_k'^{down}, p_{k-1})p_{k-1}
\end{aligned}
$$

$$
\begin{aligned}
\partial' t_k^{up} &= \sum \alpha(t_k^{up}, t_{k-1}^{up})t_{k-1}^{up} \\
&+ \sum \alpha(t_k^{up}, q_{k-1}^{up})q_{k-1}^{up}
\end{aligned}
$$

$$
\begin{aligned}
\partial' t_k'^{down} &= \sum \alpha(t_k'^{down}, t_{k-1}'^{down})t_{k-1}'^{down} \\
&+ \sum \alpha(t_k'^{down}, q_{k-1}'^{down})q_{k-1}'^{down} \\
&+ \sum \alpha(t_k'^{down}, p_{k-1})p_{k-1}
\end{aligned}
$$

These sums extend over all the elements on the right hand side and α is the number of gradient flow lines (mode 2) between the corresponding critical points. We want to prove $\partial'^2 = 0$ over $C_k(Y)$ by equating ∂' with the boundary operator ∂^M of Floer theory which is of the form $\partial^M(s_k) = \sum \alpha(s_k, s_{k-1})s_{k-1}$ for a gradient vector field and counts the number of gradient flow lines α (mod 2) between two rest points with relative index difference one, without any partitioning on the set of isolated rest points s_k of index k. In our case, we have

such a partitioning and therefore more refined relationships in the definition of ∂'. And then, for all the generators of $C_*(Y)$, $\partial' = \partial^M$; we show this equality for $p_k, q_k^{up}, t_k'^{down}$ as for the other cases it can be similarly proved.

If we consider such a partitioning on the set of rest points of our vector field we have:

$$
\begin{aligned}
\partial^M(p_k) &= \sum \alpha(p_k, p_{k-1})p_{k-1} + \sum \alpha(p_k, q_{k-1}^{up})q_{k-1}^{up} \\
&+ \sum \alpha(p_k, q_{k-1}'^{down})q_{k-1}'^{down} + \sum \alpha(p_k, t_{k-1}^{up}).t_{k-1}^{up} \\
&+ \sum \alpha(p_k, t_{k-1}'^{down})t'^{down}
\end{aligned}
$$

;

comparing this formula with that of $\partial' p_k$ we see that we have two extra terms in the latter; as we have explained after the definition of ∂, the 3th and the 5th term are not present in the former case. To have $\partial^M(q_k^{up}) = \partial'(q_k^{up})$, the three coefficients

$$
\alpha(q_k^{up}, q_{k-1}'^{down}), \alpha(q_k^{up}, t_{k-1}'^{down}), \alpha(q_k^{up}, p_{k-1})
$$

need to be zero. The first one is zero since there are exactly two gradient flow lines (heteroclinic orbits) from q_k^{up} to $q_{k-1}'^{down}$ which correspond to replacement of an orbit O_{k-1}. We note that for the other $q_{k-1}'^{down}$ coming from other orbits α is zero by definition of ∂ over $C_k(X)$ as otherwise in X we would have flow lines between two orbits of the same index which is not possible by the Morse-Smale condition. For the same reason, the second element is also zero since there is no flow line from q_k^{up} to $t_{k-1}'^{down}$. Also the last α is zero as otherwise there would be flow lines from a periodic orbit of index $k-1$ to an isolated rest point with index $k-1$ in X, again violating Morse-Smale.

Finally $\partial^M(t_k'^{down}) = \partial'(t_k'^{down})$ if we show that $\alpha(t_k'^{down}, t_{k-1}^{up})$ and $\alpha(t_k'^{down}, q_{k-1}^{up})$ are zero. If not, there would be two orbits in X with index difference two which are the boundaries of a cylinder, which is not possible.

Therefore over $C_*(Y)$, $\partial^M = \partial'$ and hence $\partial'^2 = 0$ by classical Morse-Floer theory.

3. We now define $\varphi_* : C_*(X) \longrightarrow C_*(Y)$. For $0 \leq k \leq m$, we put

$$
\varphi_*(p_k) = p_k, \quad \varphi_*(O_k^0) = q_k'^{down}, \quad \varphi_*(O_{k-1}^1) = q_k^{up},
$$
$$
\varphi_*(H_k^0) = t_k'^{down}, \quad \varphi_*(H_{k-1}^1) = t_k^{up}.
$$

φ_* is an isomorphism by the above construction of the rest points of Y. To prove φ_* is a chain map from $C_*(X)$ to $C_*(Y)$, we should have $\partial'\varphi_* = \varphi_*\partial$. Here, we show this equality for one of the generators of $C_k(X)$ and for the others it can be similarly obtained. For O_{k-1}^1
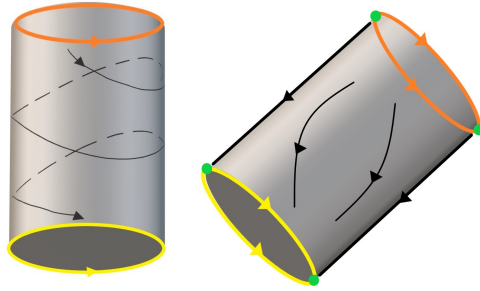
Figure 2.2

we have:

$$\varphi_*\partial(O^1_{k-1}) = \varphi_* \left(\sum \alpha(O_{k-1}, O_{k-2}).O^1_{k-2} + \sum \alpha(O_{k-1}, H_{k-2}).H^1_{k-2} \right)$$
$$= \sum \alpha(q^{up}_k, q^{up}_{k-1}).q^{up}_{k-1} + \sum \alpha(q^{up}_k, t^{up}_{k-1}).t^{up}_{k-1}$$
$$= \partial' q^{up}_k$$
$$= \partial' \varphi_*(O^1_{k-1})$$

Therefore $\partial'\varphi_* = \varphi_*\partial$ and since $\partial'^2 = 0$ and $\partial^2 = \varphi_*^{-1}\partial'^2\varphi_*, \partial^2 = 0$ $\qquad\square$

We can then define $\mathbb{Z}_2$ Morse-Floer homology of M by putting for each $k, 0 \le k \le m$,

$$H_k(M, \mathbb{Z}_2) = \frac{ker(\partial_k)}{image(\partial_{k+1})}.$$

Remark 2.2.5. *Although here we do not treat orientations, we observe from the following figure that in the above equalities φ_* preserves the parity of α as each connected component of $M(O_{k-1}, O_{k-2})$ corresponds to exactly one gradient flow line from q^{up}_k to q^{up}_{k-1} (and exactly one flow line from q'^{down}_{k-1} to q'^{down}_{k-2}). Similarly the same happens when we consider connected components of $M(O_{k-1}, H_{k-2})$.*

2.3 Computing Homology Groups of Smooth Manifolds

We shall now illustrate the simple computation of Floer homology for some smooth vector fields.

1. Let the sphere S^2 be equipped with a vector field V which has two isolated rest points of index zero at the north (N) and the south (S) pole, and one periodic orbit O of index one on the equator. Then

$$
\begin{aligned}
C_2 &= \left(O_1^1\right) \\
C_1 &= \left(O_1^0\right) \\
C_0 &= (N_0, S_0)
\end{aligned}
$$

$\partial_2 O_1^1 = 0$ since there is no closed orbit of index 0 and therefore O_1^1 is the only generator for $H_2(S^2, \mathbb{Z}_2)$. $\partial_1 O_1^0 = \alpha(O_1, N_0).N_0 + \alpha(O_1, S_0).S_0 = N_0 + S_0 \neq 0$ and therefore O_1^0 does not contribute to $H_1(S^2, \mathbb{Z}_2)$ and $H_1(S^2, \mathbb{Z}_2) = 0$. $\partial_0 N_0 = 0 = \partial_0 S_0$ but since $N_0 + S_0$ is in the im-

Figure 2.3

age of ∂_1 therefore we have a single generator for $H_0(S^2, \mathbb{Z}_2)$.

2. If we reverse the orientation of flow lines in the previous example, the isolated rest points at the north and south pole will get index two and the index of the periodic orbit becomes zero. Therefore:

$$
\begin{aligned}
C_2 &= (N_2, S_2) \\
C_1 &= \left(O_0^1\right) \\
C_0 &= \left(O_0^0\right)
\end{aligned}
$$

Figure 2.4

$\partial_2 N_2 = O_0^1 = \partial_0 S_2$ and $N_2 - S_2$ is the generator for $H_2(S^2, \mathbb{Z}_2)$.

Also $\partial_1 O_1^1 = 0$ but since O_1^1 is in the image of ∂_2 it does not contribute to $H_1(S^2, \mathbb{Z}_2)$. Finally $\partial_0 O_0^0 = 0$ and therefore O_0^0 is the only generator for $H_0(S^2, \mathbb{Z}_2)$.

3. Consider S^2 as following with a vector field V which has two isolated rest points, at the north pole of index zero and at the south pole of index two, one orange homoclinic orbit H of index one and one yellow periodic orbit O of index zero.

$$
\begin{aligned}
C_2 &= \left(S_2, H_1^1\right) \\
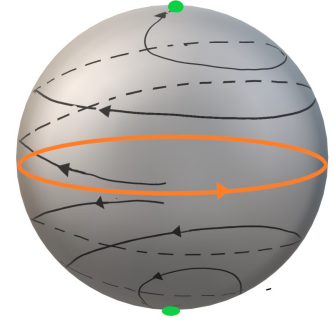C_1 &= \left(H_1^0, O_0^1\right) \\
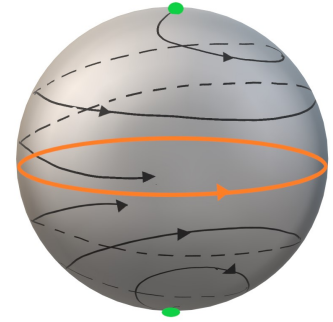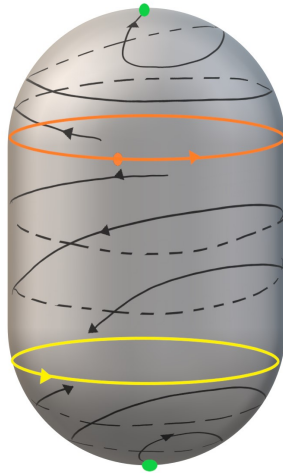C_0 &= \left(O_0^0, N_0\right)
\end{aligned}
$$

Figure 2.5

$\partial_2 S_2 = O_0^1 = \partial_2 H_1^1$ and therefore $S_2 - H_1^1$ is the only generator for $H_2(S^2, \mathbb{Z}_2)$. $\partial_1 H_1^0 = \alpha(H_1, O_0).O_0^0 + \alpha(H_1, N_0).N_0 = O_0^0 + N_0 \neq 0$

and therefore H_1^0 does not contribute to $H_1(S^2, \mathbb{Z}_2)$. On the other hand, $\partial_1 O_0^1 = 0$ but since O_0^1 is in the image of ∂_2 it does not contribute to $H_1(S^2, \mathbb{Z}_2)$ and therefore $H_1(S^2, \mathbb{Z}_2) = 0$. $\partial_0 N_0 = 0 = \partial_0 O_0^0$ but since $O_0^0 + N_0$ is in the image of ∂_1 therefore we have just one generator for $H_0(S^2, \mathbb{Z}_2)$.

4. Finally, a two dimensional Torus T^2 with a vector field V with two periodic orbits O_1 and O_0':
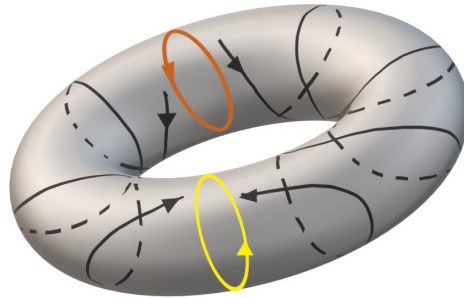

Figure 2.6

$$C_2 = \left(O_1^1\right)$$
$$C_1 = \left(O_1^0, O_0'^1\right)$$
$$C_0 = \left(O_0'^0\right)$$

$\partial_2 O_1^1 = 2.O_0'^1 = 0$ therefore O_1^1 is the generator for $H_2(T^2, \mathbb{Z}_2)$.

$\partial_1 O_1^0 = 2.O_0^{\prime 0} = 0$ so O_1^0 is a generator for $H_1(T^2, Z)$. Also $\partial_1 O_0^{\prime 1} = 0$ and therefore $O_0^{\prime 1}$ is another generator for $H_1(T^2, \mathbb{Z}_2) = 0$.

Finally $\partial_0 O_0^{\prime 0} = 0$ and therefore we have one generator for $H_0(T^2, \mathbb{Z}_2)$.

Remark 2.3.1. *For a computation of the homology groups of the first two examples via Morse- Bott theory (after turning the periodic orbits into critical submanifolds of a gradient flow), see [4].*

3

Floer Homology of (Forman's) combinatorial vertor fields

In this chapter, we want to present a type of Floer boundary operator on CW complexes which provide a natural way of describing spaces combinatorially, preserving their homotopy types. Forman introduced the notion of a combinatorial dynamical system on CW complexes [23]. He developed discrete Morse theory for the gradient vector field of a combinatorial Morse function and studied the homological properties of its dynamic [25] . For the general combinatorial vector fields where as opposed to gradient vector fields, the chain recurrent set might also include closed paths, he studied some homological properties by generalizing the combinatorial Morse inequalities. It remains, however, to construct a Floer type boundary operator for these general combinatorial vector fields. We define a Morse-Floer boundary operator for combinatorial vector fields on a finite simplicial complex. With this tool we no longer need a Morse function to compute the Betti numbers of the complex. Combinatorial vector fields can be considered as the combinatorial version of smooth Morse-Smale dynamical systems on finite dimensional manifolds; here in contrast to the smooth case we cannot have homoclinic points and homoclinic orbits as here, we cannot have a continuous bifurcation between a pair of heteroclinic orbits and a closed one, and in particular none with a homoclinic orbit in the middle.

3.1 Preliminaries

We now recall some of the main definitions that Forman introduced. Let M be a finite CW complex of dimension m, with K the set of open cells of M and K_p the set of cells of dimension p. If σ and τ are two cells of M, we write σ_p if $\dim(\sigma) = p$, and $\sigma < \tau$ if $\sigma \subseteq \overline{\tau}$ where $\overline{\tau}$ is the closure of τ and we call σ a face of τ.

Suppose σ_p is a face of τ_{p+1}, B a closed ball of dimension $p + 1$ and $h : B \to M$ the characteristic map for τ i.e., a homeomorphism from the interior of B onto τ.

Definition 3.1.1. σ_p *is a* regular face *of* τ_{p+1} *if*

- $h^{-1}(\sigma) \to \sigma$ *is a homeomorphism.*

- $\overline{h^{-1}(\sigma)}$ *is a closed p-ball.*

Otherwise we say σ is an *irregular face* of τ. If M is a regular CW complex (such as a simplicial or a polyhedral complex) then all its faces are regular.

Definition 3.1.2. *A combinatorial vector field on M is a map $V : K \to K \cup 0$ such that*

- *For each p, $V(K_p) \subseteq K_{p+1} \cup 0$.*

- *For each $\sigma_p \in K_p$, either $V(\sigma) = 0$ or σ is a regular face of $V(\sigma)$.*

- *If $\sigma \in \mathrm{Image}(V)$ then $V(\sigma) = 0$.*

- *For each $\sigma_p \in K_p$*
  $\sharp\{u_{p-1} \in K_{p-1} \mid V(u) = \sigma\} \leq 1.$

To present the vector field on M for any $\sigma \in K$ where $V(\sigma) \neq 0$ we usually draw an arrow on M whose tail begins at σ and extend this arrow into $V(\sigma)$. Thus, for each simplex σ_p, there are precisely 3 disjoint possibilities:

- σ is the head of an arrow $(\sigma \in Image(V))$.

- σ is the tail of an arrow $(V(\sigma) \neq 0)$.

- σ is neither the head nor the tail of any arrow $(V(\sigma) = 0$ and $\sigma \notin \mathrm{Image}(V)$;

In the last case we call such a σ_p a zero or rest point of V of index p. Cells which are not rest points occur in pairs $(\sigma, V(\sigma))$ with $\dim V(\sigma) = \dim \sigma + 1$. From now on and for simplicity we restrict ourselves to the special case of simplicial complexes, instead of CW complexes. As the combinatorial version of closed periodic orbits in smooth manifolds we have the next definition:

Definition 3.1.3. *Define a V-path of index p to be a sequence*
$\gamma : \sigma_p^0, \tau_{p+1}^0, \sigma_p^1, \tau_{p+1}^1, ..., \tau_{p+1}^{r-1}, \sigma_p^r$
  such that for all $i = 1, ..., r - 1$:
$V(\sigma^i) = \tau^i$ *and* $\sigma^i \neq \sigma^{i+1} < \tau^i.$
A closed path γ of length r is a V-path such that $\sigma_p^0 = \sigma_p^r$. Also γ is called non-stationary *if $r > 0$. In particular we define the* index *of a simplex σ_p to be its dimension p.*

Forman showed that there is an equivalence relation on the set of closed paths by considering two paths γ and γ' to be equivalent if γ is the result of varying the starting point of γ'. An equivalence class of closed paths of index k will be called a *closed orbit* of index k and denoted by O_k.

Definition 3.1.4. *The combinatorial chain recurrent set $R(V)$ for a combinatorial vector field V on M is defined to be the set of simplices σ_p which are either rest points of V or are contained in some non-stationary closed path γ (γ must have index either $p - 1$ or p).*

The chain recurrent set can be decomposed into a disjoint union of basic sets $R(M) = \cup_i \Lambda_i$ where two simplices $\sigma, \tau \in R(V)$ belong to the same basic set if and only if there is a closed non-trivial V-path γ which contains both σ and τ. Forman proved that if there are no non-stationary closed paths, then V is the combinatorial negative gradient vector field of a combinatorial Morse function. However when V has closed paths, then it cannot be the gradient of a function. Subsequently he defined a combinatorial "Morse-type" function on K, called a Lyapunov function, which is constant on each basic set, and has the property that, away from the chain recurrent set, V is the negative gradient of f.

Remark 3.1.5. *This Lyapunov function can be considered as the combinatorial analogue of the Morse-Bott energy function which Mayer defined for Morse-Smale dynamical systems.*

3.2 The chain complex of combinatorial vector fields

Forman obtained Morse-type inequalities based on the basic sets of V and showed that these sets control the topology of M [23]. In this section, we present a direct way of recovering the homology of the underlying complex from the chain recurrent set of a combinatorial vector field on M from our Floer type boundary operator; this operator acts on chain groups generated by the basic sets and counts the number of suitable V-paths between elements of the chain recurrent set. We consider V to be a combinatorial vector field on a finite simplicial complex M.

We define the Morse-Floer complex of V denoted by $(M, C_*(V), \partial)$ as follows. Let C_k denote the finite vector space (with coefficients in $\mathbb{Z}_2$) generated by the set of rest points p_k and closed orbits O_{k-1} of the vector field:

$$\left(p_k, O_{k-1}^1, O_k^0\right)$$

in which by O_{k-1}^1 we mean the whole closed orbit O_{k-1} of index $k-1$ and by O_k^0 we mean an arbitrary simplex with dimension k in the closed orbit O_k. Similar to the smooth case, each such orbit carries topology in two adjacent dimensions, namely a closed orbit O_k generates an element O_k^1 in C_{k+1} and an element O_k^0 in C_k. We note that here, by definition of combinatorial vector fields, we do not have any V-path between the elements of the same C_k; but in order to get a Floer type boundary operator in the same way as in the smooth setting we have to exclude three different cases in our vector field; we assume:

1. There is no V-path from a face of a critical simplex p_k to a $(k-1)$-dimensional simplex in an orbit O_{k-1}.

2. There is no V-path from a face of a k-dimensional simplex of an orbit of index $k-1$ to a critical simplex of dimension $k-1$.

3. There is no V-path from a face of a k-dimensional simplex of an orbit of index $k-1$ to a $(k-1)$-dimensional simplex of another orbit of index $k-1$.

This will be used in the proof of Thm. 3.2.1. In the smooth setting, the excluded cases cannot occur because of the Morse-Smale transversality condition.

To be able to define the combinatorial Floer-type boundary operator, we have to transfer the idea of number of connected components of the moduli spaces of flow lines to our combinatorial setting. As we saw, the number of these components (mod 2) plays a key rule in the definition of the boundary operator in the smooth setting. In the following for two simplices of the same dimension q and q' by $q \perp q'$ we mean that q and q' are lower adjacent, i.e., they have a common face.

We have V-paths between closed orbits and rest points which make different following cases: For two orbits O_{k-1} and O_{k-2} we define the set $VP(O_{k-1}, O_{k-2})$ as the set of all V-paths starting from the faces of $k-1$ and k-dimensional simplices of O_{k-1} and go to respectively $k-2$ and $k-1$ dimensional simplices of O_{k-2}.

If $VP(O_{k-1}, O_{k-2})$ is non-empty, for O_{k-1}^1 and O_{k-2}^1, we define the higher dimensional spanned set of V-paths in $VP(O_{k-1}, O_{k-2})$, denoted by $SVP(O_{k-1}^1, O_{k-2}^1)$ to be

$$\{q \in K_k, q \in Image(V) \mid \exists \gamma \in VP(O_{k-1}, O_{k-2}), q \in \gamma\}.$$

On this set we can then define a relation as follows. We say q and q' in $SVP(O_{k-1}^1, O_{k-2}^1)$ are related ($q \sim q'$) if q and q' belong respectively to two V-paths $\gamma : \alpha_{k-1}^0, ..., q_k, ..., \alpha_{k-1}^r$ and $\gamma' : \beta_{k-1}^0, ..., q_k', ..., \beta_{k-1}^s$ where α_{k-1}^0 and β_{k-1}^0 are faces of k-dimensional simplices of O_{k-1} and α_{k-1}^r and β_{k-1}^s are some $k-1$ dimensional simplices in O_{k-2} such that one of the following situations happens:

- Either α_{k-1}^0 and β_{k-1}^0 coincide (and therefore γ and γ' are the same) or

- $\alpha_{k-1}^0 \perp \beta_{k-1}^0$ or

- There is a sequences of $k-1$ dimensional simplices $\theta_{k-1}^0, ...\theta_{k-1}^z$, where $\theta_{k-1}^0, ...\theta_{k-1}^z$ are the faces of k dimensional simplices in O_{k-1} such that $\alpha_{k-1}^0 \perp \theta_{k-1}^0$, $\beta_{k-1}^0 \perp \theta_{k-1}^z$ and for each i, $\theta_{k-1}^i \perp \theta_{k-1}^{i+1}$ and θ_{k-1}^i is the starting simplex of some $\gamma \in VP(O_{k-1}, O_{k-2})$.

It is straightforward to check that $\sim$ is an equivalence relation on $SVP(O_{k-1}^1, O_{k-2}^1)$. On the other side for two arbitrary simplices of dimension $k-1$ and $k-2$ in respectively O_{k-1} and O_{k-2} we consider the following equivalence relation($\sim'$) on $SVP(O_{k-1}^0, O_{k-2}^0)$:

$$\{q \in K_{k-1}, q \in Image(V) \mid \exists \gamma \in VP(O_{k-1}, O_{k-2}), q \in \gamma\}.$$

We say q and q' in $SVP(O_{k-1}^0, O_{k-2}^0)$ are related ($q \sim' q'$) if there are w and w' in $SVP(O_{k-1}^1, O_{k-2}^1)$ such that $q < w$ and $q' < w'$ and $w \sim w'$. By definition $\sim'$ is also

an equivalence relation on $SVP(O_{k-1}^0, O_{k-2}^0)$ and the number of its equivalence classes is exactly the number of equivalence classes of $\sim$ over $SVP(O_{k-1}^1, O_{k-2}^1)$.

For instance consider the following triangulation of the torus which has two closed orbits of index one and index zero, respectively shown by green and red arrows. Here, $SVP(O_{k-1}^1, O_{k-2}^1)$ is the set of all the two dimensional coloured simplices and based on the above equivalence relation, this set is partitioned into two sets of yellow and pink two dimensional simplices. Also $SVP(O_{k-1}^0, O_{k-2}^0)$ is the set of all marked (with cross sign) edges which is partitioned into two sets, represented by orange and purple signs.
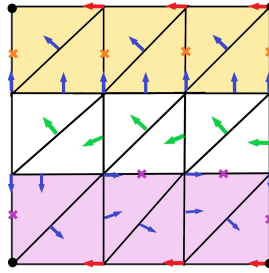
Figure 3.1

If for two orbits, O_{k-1} and O_{k-2}, $VP(O_{k-1}, O_{k-2})$ is empty and some of the faces of O_{k-1} (faces of both $k-1$ and k-dimensional simplices) coincide with $k-2$ and $k-1$ dimensional simplices in O_{k-2}, we say O_{k-2} is attached to O_{k-1}. In the tetrahedron shown below the bottom faces of the closed red orbit of index one, is the closed orbit of index zero with purple arrows
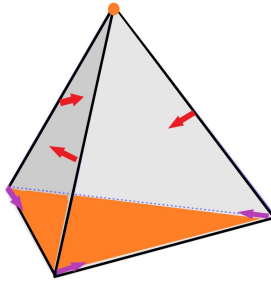

Figure 3.2

Also we could have V-paths, $VP(p_k, O_{k-2})$, from the faces of a critical simplex p_k of index k which go to the $k-1$ dimensional simplices of some orbit of index $k-2$; we define the span set of these V-paths, denoted by $SVP(p_k, O_{k-2}^1)$ to be

$$SVP(p_k, O_{k-2}^1) := \{q \in K_k, q \in Image(V) \mid \exists \gamma \in VP(p_k, O_{k-2}), q \in \gamma\}.$$

As above we can define an equivalence relation on this set in which the equivalence classes are obtained based on the following relation:

$q \sim q'$ if they belong respectively to two V-paths $\gamma : \alpha_{k-1}^0, ..., q_k, ..., \alpha_{k-1}^r$ and $\gamma' : \beta_{k-1}^0, ..., q_k', ..., \beta_{k-1}^s$ such that either α_{k-1}^0 and β_{k-1}^0 coincide or $\alpha_{k-1}^0 \perp \beta_{k-1}^0$ or there

is a sequence of $k-1$ dimensional simplices $\theta_{k-1}^0, ... \theta_{k-1}^z$, where $\theta_{k-1}^0, ... \theta_{k-1}^z$ are the faces of p_k such that $\alpha_{k-1}^0 \perp \theta_{k-1}^0$, $\beta_{k-1}^0 \perp \theta_{k-1}^z$ and for each i, $\theta_{k-1}^i \perp \theta_{k-1}^{i+1}$. We note that here, α_{k-1}^0 and β_{k-1}^0 are faces of p_k and α_{k-1}^r and β_{k-1}^s are some $k-1$ elements of O_{k-2}.

Also for V on M, for some rest point p_k and some closed orbit O_{k-2}, the faces of p_k and $k-1$ dimensional simplices in O_{k-2} might coincide. In the above tetrahedron where the faces of orange 2-d rest simplex coincides with the one dimensional simplices in the closed orbit of index zero with purple arrows. We consider this again as an *attachment*.

In the third possible case, V-paths start from the faces of k-dimensional simplices of a closed orbit of index k, O_k, and go to a rest simplex of index $k-1$, p_{k-1}. We denote the set of such V-paths by $VP(O_k, p_{k-1})$ and we consider $SVP(O_k^0, p_{k-1}) := \{q \in K_k, q \in Image(V) \mid \exists \gamma \in VP(O_k, p_{k-1}), q \in \gamma\}$. In this set we call two simplices q and q' equivalent if either q and q' coincide or $q \perp q'$ or we can find a sequence of simplices in $SVP(O_k^0, p_{k-1})$ such as $\theta_{k-1}^0, ... \theta_{k-1}^z$, such that $q \perp \theta_{k-1}^0$, $q' \perp \theta_{k-1}^z$ and for each i, $\theta_{k-1}^i \perp \theta_{k-1}^{i+1}$. Here we have to exclude p_{k-1} for determining lower adjacency of k-dimensional simplices in $SVP(O_k^0, p_{k-1})$, namely if $q \cap q' = p_{k-1}$, they belong to different classes. As an example consider the following triangulation for the torus with four orange rest simplices, one of index two, two of index one and another one of index zero, and a closed red orbit of index one. Here, the edges marked by cross signs are the edges in $SVP(O_1^0, p_0)$, which is portioned into two pink and yellow marked edges. If $VP(O_k, p_{k-1})$ is empty, but O_k and p_{k-1} have a non-empty intersection, we have another type of attachment. For an example of this case see the top critical vertex and the red O_1 in the above tetrahedron.
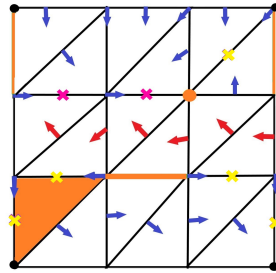

Figure 3.3

Finally if we substitute O_k^0 in the third case by a rest point of index k, p_k, we count the number of equivalence classes of $SVP(p_k, p_{k-1}) := \{q \in K_k, q \in Image(V) \mid \exists \gamma \in VP(p_k, p_{k-1}), q \in \gamma\}$ where $VP(p_k, p_{k-1})$ is the set of all V-paths starting from the faces of p_k and go to p_{k-1} by passing through k-dimensional simplices, based on the following relation:

We say q and q' in $SVP(p_k, p_{k-1})$ are related ($q \sim q'$) if there is a V-path in $VP(p_k, p_{k-1})$ which includes both q and q'. Therefore the number of equivalence classes here is the number of V-paths starting from the faces of p_k which go to p_{k-1}.

The differential $\partial_k : C_k(V) \longrightarrow C_{k-1}(V)$ counts the number of the above equivalence classes mod 2, denoted by α, and for the three types of attachments we consider $\alpha = 1$. That is,

$$
\begin{aligned}
\partial p_k &= \sum \alpha(p_k, p_{k-1}) p_{k-1} + \sum \alpha(p_k, O^1_{k-2}) O^1_{k-2} \\
\partial O^0_k &= \sum \alpha(O^0_k, O^0_{k-1}) O^0_{k-1} + \sum \alpha(O^0_k, p_{k-1}) p_{k-1} \\
\partial O^1_{k-1} &= \sum \alpha(O^1_{k-1}, O^1_{k-2}) O^1_{k-2}
\end{aligned}
$$

where the sums extend over all the elements on the right hand side; for instance the second sum in the first line is over all closed orbits O^1_{k-2} of index $k-2$. In Forman's discrete Morse theory where there is no closed orbit (and therefore the combinatorial vector field is the gradient of a discrete Morse function), $\alpha(p_k, p_{k-1})$ is the number of gradient V-paths from the faces of the rest point p_k of higher dimension to the rest point of lower dimension p_{k-1} (in this case all the coefficients in the above formula except the first coefficient in the first line are zero).

Also in the above definition, $\alpha(O^0_k, O^0_{k-1}) = \alpha(O^1_k, O^1_{k-1})$ as in the left side the k and $k-1$ dimensional simplices are chosen arbitrarily from their orbits. On the other hand, similar to the smooth case we do not have terms with coefficients of the form $\alpha(p_k, O^0_{k-1})$ in the definition of the boundary operator. This will be used in the proof of Thm. 3.2.1. If there were a V-path from the faces of some p_k to some O^0_{k-1}, then we would be able to consider V-paths to the corresponding O^1_{k-1} which comes from the same closed orbit. But O^1_{k-1} and p_k belong to the the same C_k which contradicts our main assumption on chain groups.

Theorem 3.2.1. $\partial^2 = 0$.

To prove this theorem similarly to Theorem 2.2.4 in the smooth case, we introduce a procedure to replace any closed path of index p (correspondingly its orbit of index p, O_p) by a rest point of index p and one of index $p+1$ which are joined by two gradient V-paths starting from the faces of a higher dimensional rest point and going to the lower dimensional rest point.

We assume V has a finite number of closed non-stationary paths (orbits) and rest simplices. Choose arbitrarily one of these closed paths γ of index p, $\gamma : \sigma^0_p, \tau^0_{p+1}, \sigma^1_p, \tau^1_{p+1}, ..., \tau^{r-1}_{p+1}, \sigma^r_p = \sigma^0_p$. γ is a sequence of p and $(p+1)$ dimensional simplices. Take one of the $p+1$ dimensional simplices τ^k_{p+1} where $k \neq r-1$. (Note that for non-stationary closed paths such a τ^k always exists). We consider the following two sets of the simplices of γ by preserving the orders in each of the sets:

$$
\begin{aligned}
&\sigma^0_p, ..., \tau^{k-1}_{p+1}, \sigma^k_p, \tau^k_{p+1} \text{ and} \\
&\tau^k_{p+1}, \sigma^{k+1}_p, \tau^{k+1}_{p+1}, ..., \sigma^r_p = \sigma^0_p
\end{aligned}
$$

where the union of the elements in these sets consists of all the simplices of γ and their intersection is the starting simplex of the closed path σ_p^0 and the one of higher dimension that we took τ_{p+1}^k.

We keep the arrows in the second set as they are in γ and in the first set we reverse the direction of V-path from σ_p^0 to τ_{p+1}^k. Namely instead of a pair such as $(\sigma_p^s, \tau_{p+1}^s)$ in γ (for $0 \le s \le k$) we will have $(\sigma_p^s, \tau_{p+1}^{s-1})$ in our vector field where the two simplices σ_p^0 and τ_{p+1}^k will no longer be the tail and head of any arrow; therefore by definition both of them become rest points and there is no other rest point in γ created in this process. We note that in this procedure we just change the arrows in O and the other pairs of the vector field (outside O) are not changed.

Proof. of theorem 3.2.1. If by the help of above procedure we replace all the closed paths (orbits) by two rest points whose indices (dimensions) differ by one we get a vector field V' which has no closed path (orbit) and therefore there is a discrete Morse function on M whose gradient is V'. V' has all the rest points of V and two rest points q_k^{up} (the simplex of higher index) and $q_{k-1}'^{down}$ (the simplex of lower index) instead of every orbit O_{k-1} of index $k-1$. Then we have the following three steps to prove the theorem:

1. We consider $C_k(V')$ to be the finite vector space (with coefficients in $\mathbb{Z}_2$) generated by

$$\left(p_k, q_k^{up}, q_k'^{down} \right)$$

   where in this set q_k^{up} comes from an orbit of index $k-1$ and $q_k'^{down}$ comes from the replacement of an orbit of index k.

2. we define a boundary operator ∂' and consequently a chain complex corresponding to $(V', C_*(V'), \partial')$.

3. Then we prove there is an isomorphism (chain map) $\varphi* : C_*(V) \longrightarrow C_*(V')$.

Since $\varphi*$ is an isomorphism we get our desired equality $\partial^2 = 0$ as $\partial = \varphi^{-1}\partial'$ and $\partial^2 = \varphi^{-1}\partial'^2$.

1. All the elements of the chain recurrent set of V' are rest simplices and for each index k they can be partitioned into three different sets $p_k, q_k^{up}, q_k'^{down}$. Here, in contrast to the smooth case, orbits and rest points can have non-empty intersections; in particular for the three types of attachments, the pairwise intersections are non-empty. However partitioning of rest simplices is possible since the indices of the rest simplices are the same as their dimensions and after converting orbits into two rest simplices, they will belong to different chain groups (in adjacent dimensions).

2. We define $\partial' : C_k(V') \longrightarrow C_{k-1}(V')$ as follows:

$$
\begin{aligned}
\partial' p_k &= \sum \alpha(p_k, p_{k-1}).p_{k-1} + \sum \alpha(p_k, q^{up}_{k-1}).q^{up}_{k-1} \\
\partial' q^{up}_k &= \sum \alpha(q^{up}_k, q^{up}_{k-1}).q^{up}_{k-1} \\
\partial' q'^{down}_k &= \sum \alpha(q'^{down}_k, q'^{down}_{k-1}).q'^{down}_{k-1} \\
&+ \sum \alpha(q'^{down}_k, p_{k-1}).p_{k-1}
\end{aligned}
$$

To prove $\partial'^2 = 0$ over $C_k(V')$, we want to equate ∂' with the discrete Morse-Floer boundary operator ∂^M of a combinatorial gradient vector field of the form $\partial^M(s_k) = \sum \alpha(s_k, s_{k-1}).s_{k-1}$. There we count the number of gradient V-paths α (mod 2) between two rest points of relative index difference one without any such partitioning on the set of rest simplices s_k of index k. In our case where we have such kind of partitioning we should show that for all the generators of $C_*(V')$, $\partial' = \partial^M$.

After the preceding procedure, we have:

$$
\begin{aligned}
\partial^M(p_k) &= \sum \alpha(p_k, p_{k-1}).p_{k-1} + \sum \alpha(p_k, q^{up}_{k-1}).q^{up}_{k-1} \\
&+ \sum \alpha(p_k, q'^{down}_{k-1}).q'^{down}_{k-1};
\end{aligned}
$$

comparing this formula with that of $\partial' p_k$ in the above formula we see that there is one extra term in the latter; because we exclude case (1) in our vector field, the third sum is not present in the former case.

As in the previous discussion to have $\partial^M(q^{up}_k) = \partial'(q^{up}_k)$, the following two coefficients should be zero:

$\alpha(q^{up}_k, q'^{down}_{k-1}), \alpha(q^{up}_k, p_{k-1})$. In the first case if q^{up}_k and q'^{down}_{k-1} are coming from replacement of the same orbit O_{k-1}, we will have exactly two V'-paths from the faces of q^{up}_k to q'^{down}_{k-1} and it is zero mud 2. If they are not obtained from replacement of the same orbit O_{k-1}, α is zero as otherwise in V we would have V-paths between two orbits of the same index which either contradicts the non-existence of V-paths between elements of the same chain group or violates our exclusion (3) on the vector field. On the other hand, the second α is zero as otherwise it violates our assumption (exclusion 2) on the vector field.

Finally $\partial^M(q'^{down}_k) = \partial'(q'^{down}_k)$ if $\alpha(q'^{down}_k, q^{up}_{k-1})$ is zero; if not, we would have two closed orbits O and O' in V such that the faces of O are connected to O' by some V-paths and their indices differ by two which is not possible.

Therefore on $C_*(V)$, $\partial^M = \partial'$ and $\partial'^2 = 0$ since by Morse-Floer theory for combinatorial gradient vector fields $(\partial^M)^2 = 0$.

3. We define $\varphi* : C_*(V) \longrightarrow C_*(V')$ as follows. For $0 \leq k \leq m$,

$$\varphi_*(p_k) = p_k, \quad \varphi_*(O_k^0) = q_k'^{down}, \quad \varphi_*(O_{k-1}^1) = q_k^{up}$$

φ_* is an isomorphism by the above partitioning method for the set of rest points of V'. To prove φ_* is a chain map from $C_*(V)$ to $C_*(V')$ we should have $\partial'\varphi_* = \varphi_*\partial$

Here, we show the equality for O_{k-1}^1 and for the other generators of $C_k(V)$ it can be similarly obtained:.

$$\begin{aligned}
\varphi_*\partial(O_{k-1}^1) &= \varphi_*(\sum \alpha(O_{k-1}^1, O_{k-2}^1).O_{k-2}^1 \\
&= \sum \alpha(q_k^{up}, q_{k-1}^{up}).q_{k-1}^{up} \\
&= \partial' q_k^{up} \\
&= \partial'\varphi_*(O_{k-1}^1)
\end{aligned}$$

φ_* preserves the parity of $\alpha(O_{k-1}^1, O_{k-2}^1)$ since each equivalence class of $SVP(O_{k-1}^1, O_{k-2}^1)$ corresponds to exactly one gradient V-path from q_k^{up} to q_{k-1}^{up} (and one gradient V-path from $q_{k-1}'^{down}$ to $q_{k-2}'^{down}$.

Therefore $\partial'\varphi_* = \varphi_*\partial$ and since $\partial'^2 = 0$ and $\partial^2 = \varphi_*^{-1}\partial'^2\varphi_*$, $\partial^2 = 0$ $\qquad\square$

Remark 3.2.2. *For the three types of attachments in the above equality, after replacing orbits with two rest simplices and two gradient V-paths between them, $\alpha(p_k, q_{k-1}^{up})$, $\alpha(q_k^{up}, q_{k-1}^{up})$, $\alpha(q_k'^{down}, q_{k-1}'^{down})$ are also one. For instance, in the left tetrahedron below, we have two orange rest simplices, one of index two B_2 at the bottom and one of index zero at the top T_0 and two red and purple closed orbits of indices one and zero. If we convert the red orbit into two rest simplices, marked with red crosses, one of index two R_2 and the other one of index one R_1 and similarly turn the purple orbit into two rest simplices, marked with purple crosses, one of index one P_1 and the other one of index zero P_0 (shown in the right figure), we have $\alpha(B_2, P_1) = 1$, $\alpha(R_2, P_1) = 1$ and $\alpha(R_1, P_0) = 1$.*
(Also $\alpha(R_2, R_1) = 0$, $\alpha(P_1, P_0) = 0$ and $\alpha(R_1, T_0) = 1$.)
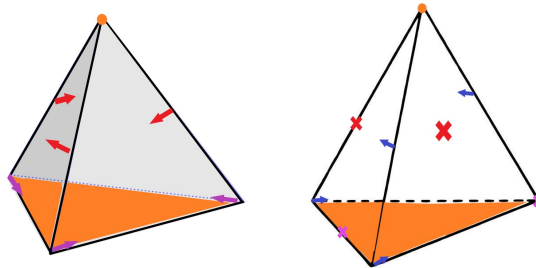

Figure 3.4

We can then define the $\mathbb{Z}_2$ Morse-Floer homology of M, for each $k, 0 \leq k \leq m$ by

$$H_k(M, \mathbb{Z}_2) = \frac{ker(\partial_k)}{image(\partial_{k+1})}$$

In [23] Forman proved Morse inequalities for general combinatorial vector fields based on his combinatorial Morse type Lyapunov function. There the main components are rest points and orbits in basic sets. Here we want to present these inequalities in a much shorter way based on the idea of changing every orbit of index $k - 1$, O_{k-1} to two rest points of index k and $k - 1$ as above. The following result can be considered as the combinatorial version of what Franks proved for smooth Morse-Smale dynamical systems [27].

Theorem 3.2.3. *Let V be a combinatorial vector field over a finite simplicial complex M with c_k rest points of index k and A_k orbits of index k. Then*

$$c_k - c_{k-1} + ... \pm c_0 + A_k \geq \beta_k - \beta k - 1 + ... \pm \beta_0,$$

where $\beta_k = \dim H_k(M, \mathbb{Z}_2)$.

Proof. We create a new vector field V' over M by replacing each closed orbit with two rest points as above. Since there is no closed orbit in V', based on what Forman showed in [25], V' is the gradient of some combinatorial Morse function on M. On the other hand, the indices of rest points do not change when turning V to V' and V' has c'_k rest points of index k where $c'_k = c_k + A_k + A_{k-1}$. Applying the Morse inequalities for gradient vector fields to c'_k in V' gives us the desired inequalities. $\square$

Remark 3.2.4. *If a simplicial complex is obtained by triangulation of a non-orientable manifold, we might not get the correct ($\mathbb{Z}_2$) homology groups when the chain recurrent set of our combinatorial vector field has non-stationary closed V-paths. However for computing the $\mathbb{Z}_2$ homology, we can turn each orbit into two rest simplices and two V-paths between them as above to get a combinatorial gradient vector field on the simplex and use the classical discrete Floer-Morse theory. For instance, consider a triangulation of the Klein bottle which has two closed orbits represented by red and blue arrows of index one and zero, respectively, as shown in the left diagram below. We note that the red orbit is twisted. Here by turning orbits into two rest simplices and two V-paths between them we get the correct $\mathbb{Z}_2$-homology of the Klein bottle which is the same as the $\mathbb{Z}_2$-homology of the triangulated torus as $\mathbb{Z}_2$-homology cannot distinguish between orientable and non-orientable surfaces.*
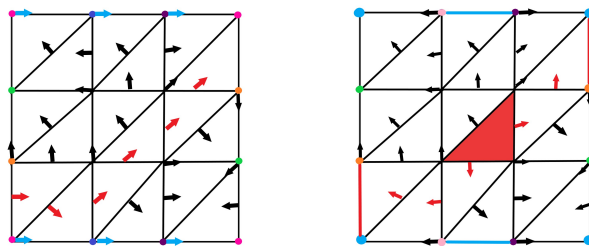

Figure 3.5

Remark 3.2.5. *Orientability of a simplicial complex is not a necessary condition for defining the Floer boundary operator for general combinatorial vector fields. For instance in the*

following diagram, we have a non-orientable simplex as each vertex is the intersection of three different edges. Here, the chain recurrent set has an orbit of index zero with red arrows, as well as three critical edges and one critical vertex in the middle. If we use theorem 3.2.1 to compute the $\mathbb{Z}_2$ homology of M based on this vector field we get $H_0(M, \mathbb{Z}_2) = 1$ and $H_1(M, \mathbb{Z}_2) = 3$.
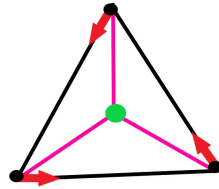

Figure 3.6

3.3 Computing Homology Groups of Simplicial Complexes

We now present the computation of Floer homology groups for some CW complexes.

1. Consider the tetrahedron as a symmetric triangulation of the Sphere S^2, equipped with a vector field V which has two rest simplices, one of index (dimension) zero (p_0) (the vertex at the top corner) and another of index two τ_2 (the simplex at the bottom), shown in orange, and a closed red orbit O_1 of index one and one of index zero O'_0 in purple. Then
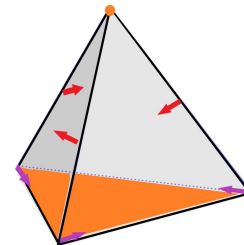
$$
\begin{aligned}
C_2 &= \left(\tau_2, O_1^1\right) \\
C_1 &= \left(O_1^0, O_0'^1\right) \\
C_0 &= \left(O_0'^0, p_0\right)
\end{aligned}
$$

Figure 3.7

$\partial_2 \tau_2 = O_0'^1$ as this is an attachment where the faces of τ_2 and edges in O_1^1 coincide. On the other hand, $\partial_2 O_1^1$ is also equal to $O_0'^1$ (another type of attachment) and therefore $\tau_2 - O_1^1$ is the only generator for $H_2(M, \mathbb{Z}_2)$.
$\partial_1 O_1^0 = \alpha(O_1^0, O_0'^0).O_0'^0 + \alpha(O_1^0, p_0).p_0 = O_0'^0 + p_0 \neq 0$ and O_1^0 does not contribute to $H_1(M, \mathbb{Z}_2)$. Also $\partial_1 O_0'^1 = 0$ but since $O_0'^1$ is in the image of ∂_2, it does not contribute to $H_1(M, \mathbb{Z}_2)$ and $H_1(M, \mathbb{Z}_2) = 0$ Finally $\partial_0 p_0 = 0 = \partial_0 O_0'^0$, but since $O_0'^0 + p_0$ is in the image of ∂_1 we have just one generator for $H_0(M, \mathbb{Z}_2)$.

2. Let T^2 at right be a triangulation of the two dimensional torus equipped with a vector field which has two closed orbits O_1 and O'_0 with green and red arrows.

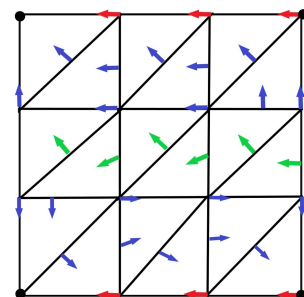Since this case is actually a discrete version of example

Figure 3.8

4 in the previous section, we have analogous structures for the chain complexes and boundaries; $SVP(O_1^1, O_0^{\prime 1})$ is partitioned into two equivalence classes and therefore $\alpha(O_1^1, O_0^{\prime 1}) = \alpha(O_1^0, O_0^0) = 0$ and all of the generators of C_k for $k = 0, 1, 2$ contribute to the corresponding homology groups.

3. Consider another combinatorial vector field on the tri-angulated torus where V has four orange rest simplices, one of index zero (p_0), a vertical edge ve_1 of index one, a horizontal edge he_1 of index one and one rest simplex τ_2 of index two and also a red orbit O of index one. We have

$$
\begin{aligned}
C_2 &= \left(\tau_2, O_1^1\right) \\
C_1 &= \left(ve_1, he_1, O_1^0\right) \\
C_0 &= \left(p_o\right)
\end{aligned}
$$
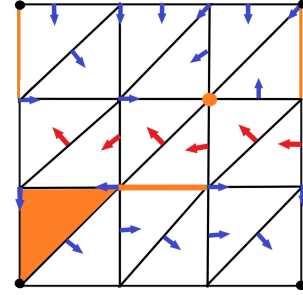
Figure 3.9

$\partial_2 \tau_2 = 1.ve_1 + 1.he_1 \neq 0$; also $\partial_2 O_1^1 = 0$ as there is no orbit of index zero here. Therefore O_1^1 is the only generator for $H_2(M, \mathbb{Z}_2)$. $\partial_1 ve_1 = 2.p_0 = 0 = \partial_1 he_1$ but since $ve_1 + he_1$ is in the image of ∂_2, $ve_1 - he_1$ is one generator for $H_1(M, \mathbb{Z}_2)$. $\partial_1 O_1^0 = 2.p_0 = 0$ and therefore O_1^0 is the other generator of $H_1(M, \mathbb{Z}_2)$. $\partial_0 p_0 = 0$ and it is the generator for $H_0(M, \mathbb{Z}_2)$.

4. Finally to compute the Floer homology groups of the depicted cube, we consider a vector field V that has two (orange and yellow) rest simplices of index two at the top τ_2^N and at the bottom τ_2^S and three different orbits, one blue orbit $(bO)_0$ of index zero, one green orbit $(gO)_0$ of index zero and a red orbit $(rO)_1$ of index one.
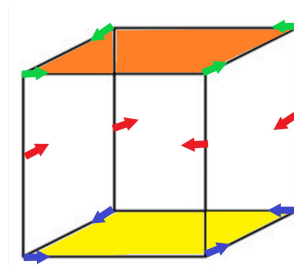
Figure 3.10

$$
\begin{aligned}
C_2 &= \left(\tau_2^N, \tau_2^S, (rO)_1^1\right) \\
C_1 &= \left((rO)_1^0, (bO)_0^1, (gO)_0^1\right) \\
C_0 &= \left((bO)_0^0, (gO)_0^0\right)
\end{aligned}
$$

$\partial_2 \tau_2^N = 1.(gO)_0^1 \neq 0$; $\partial_2 \tau_2^S = 1.(bO)_0^1 \neq 0$; $\partial_2 (rO)_1^1 = 1.(gO)_0^1 + 1.(bO)_0^1 \neq 0$ but

$\partial_2(\tau_2^N + \tau_2^S - (rO)_1^1) = 0$ and therefore we have one generator for $H_2(M, \mathbb{Z}_2)$.
$\partial_1(rO)_1^0 = 1.(bO)_0^0 + 1.(gO)_0^0 \neq 0$. $\partial_1(bO)_0^1 = 0 = \partial_1(gO)_0^1$, but since both $(bO)_0^1$ and $(gO)_0^1$ are in the image of ∂_2, we have no generator for $H_1(M, \mathbb{Z}_2)$. Finally $\partial_0(bO)_0^0 = 0 = \partial_0(gO)_0^0$, but as $(bO)_0^0 + (gO)_0^0$ is in the image of ∂_1 we have one single generator for $H_0(M, \mathbb{Z}_2)$.

Part II

Geometry and Data

4

Introduction

Principles of Network Analysis

Network analysis constitutes one of the success stories in the study of complex systems [15, 30, 44]. For the mathematical analysis, a network is modelled as a (perhaps weighted and/or directed) graph. One can then look at certain graph theoretical properties of an empirical network, like its degree or motiv distribution, its assortativity or clustering coefficient, the spectrum of its Laplacian, and so on. One can also compare an empirical network with certain deterministic or random theoretical models. Successful as this analysis clearly is, we nevertheless see two important limitations. One is that many of the prominent concepts and quantities used in the analysis of empirical networks are node based, like the degree sequence. The structure of a network is encoded, however, not in its vertices or nodes, but rather in its edges, that is, the relations between the nodes. Therefore, here we wish to advocate and pursue an analysis whose fundamental ingredients are edge based quantities. Secondly, many real data sets are naturally modelled by structures that are somewhat more general than graphs, because they may contain relations involving more than two elements. For instance, chemical reactions typically involve more than two substances. This leads to hypergraphs, a subject that is currently gaining much momentum, see for instance [16]. In an undirected graph, an edge is given by an unordered pair of vertices, that is, by a two-element subset of the set of all vertices. For an undirected hypergraph, a hyperedge is given by any non-empty subset of the vertex set. In a directed graph, an edge is an ordered pair of vertices, that is, it connects two vertices, its tail and its head. Analogously, in a directed hypergraph, a hyperedge connects two non-empty sets of vertices, a tail set and a head set. Directed graphs thus are special directed hypergraphs, where each such set contains a single vertex. Under the label of Petri nets [35], directed hypergraphs have played an important role in computer science, but withan emphasis rather on processing schemes than on network properties. As systems get larger, however, network aspects are gaining importance. Like graphs, hypergraphs can also be weighted. Let us look at some examples. In a coauthorship network, the authors are the vertices, and a set of authors constitutes a hyperedge when they coauthor a paper. Thus, coauthorship networks are naturally modelled as undirected hypergraphs. Modelling them as a graph would connect two vertices when they are part of

the set of authors of a paper. But already for three authors A, B, C, when they are pairwise connected in a graph, this cannot distinguish between the case where we have just three papers with two authors each, or whether there is a joint paper by all three of them, and perhaps in addition also some two or single author papers. Hypergraphs modelling empirical networks can also be directed. Taking the example of chemical reactions, they are typically not reversible, but rather transform a set of educts into a set of products. Thus, the task we set ourselves here is to forge tools that are powerful in the analysis of empirical networks modelled as hypergraphs. And as advocated above, such a tool should primarily evaluate properties of hyperedges rather than of vertices. Of course, once we have suitable quantities associated to hyperedges, quantities for vertices can be then also be derived, for instance by averaging over all hyperedges incident to or emanating from a vertex. So, how to go about this task? We take a conceptual approach and consider a hypergraph as a geometric object and then look for mathematical strategies for identifying invariants that can characterize geometric structures. And that leads us to one of the greatest successes in mathematics, Riemannian geometry. There, the fundamental invariants are curvatures. It might now seem that curvature is a concept only suitable for smooth structures, like smooth curves or surfaces, and therefore ill-suited for discrete structures like hypergraphs. But as it turns out, curvature concepts can be formulated more abstractly than taking second derivatives of some smooth objects. We shall now explain this in more detail, in order to motivate the approach taken in this part.

Ricci curvature: From Riemannian Geometry to Network Analysis

In Riemannian geometry (see for instance [32] as a reference), the curvature of a space quantifies its non-flatness. Among the various curvature notions that are of importance in Riemannian geometry, Ricci curvature quantifies this deviation by comparing the average distance between two sufficiently close points and the distance between two small balls around them. Bounds on curvatures can be used to connect the geometry of a Riemannian manifold with its topology, or to control stochastic processes on it. More precisely, a positive lower bound for the Ricci curvature yields the Bonnet-Myers theorem, which bounds the diameter of the space in terms of such a lower Ricci bound, the Lichnerowicz theorem for the spectral gap of the Laplacian, a control on mixing properties of Brownian motion and the Levy-Gromov theorem for isoperimetric inequalities and concentration of measures. In view of these strong implications, it is desirable to extend this to metric spaces that are more general than Riemannian manifolds. Speacifically, since such objects and properties are also meaningful and important in metric spaces that are more general than Riemannian manifolds, alternative definitions of Ricci curvatures have been proposed that are formulated in terms of local quantities and no longer depend on taking derivatives. In particular, Yann Ollivier [45] defined a notion of Ricci curvature on metric spaces equipped with a Markov chain, and extended some of the mentioned results for positively curved manifolds. His definition compares the Wasserstein distance between probability measures supported in

the neighborhoods of two given points with the distance between these points. The Wasser-stein distance between two probability measures is defined as the minimal cost needed for transporting one into the other. That is, an optimal transport problem has to be solved. – On Riemannian manifolds, this recovers the original notion of Ricci curvature (up to some scaling factor), and at the same time, it naturally applies to discrete metric spaces like graphs. Recently, this curvature has been applied in network analysis, to determine spreading or local clustering in networks modelled as undirected or directed graphs, see for instance [50]. It is therefore desirable to have such a tool also for hypergraphs. In the next chapter, we shall develop a notion of an Ollivier-type Ricci curvature for, possibly directed and/or weighted, hypergraphs [13]. There have been some prior proposals for extensions of Ollivier-Ricci curvature in such a direction (see for instance [1, 2, 57]), but our approach is more general and, as we argue, also more natural both in terms of its conceptual motivation and its range of applicability to empirical networks. From a geometric perspective, the fundamental principle that curvature characterizes types of spaces also applies here as we can distinguish and classify particular classes of directed hypergraphs in terms of their curvature. A definion of the Ollivier Ricci curvature of directed graphs was firstly proposed and investigated in [57] where out-out directions for assigning measures are used. For that, however, one needs to assume strong connectivity of the underlying directed graphs in order to find transportation plans with finite cost, but this does not hold in many real directed networks. Therefore, here, we work with in-out directions, which does not require such a strong assumption. The resulting theory is rather different from that of [57]. The first extension of the notion of Ollivier Ricci curvature to hypergraphs was proposed in [1], using a multi-marginal optimal transport problem to define curvature. Because of that, the resulting curvature in the end is an analogue of Riemannian scalar rather than Ricci curvature. Also, it does not directly apply to directed hypergraphs. We therefore propose a notion of directed hypergraph curvature that extends Ricci curvature rather than scalar curvature [13]. Since in our setting, hyperedges are directed and each direction separates the vertices of the hyperedge into two classes, similar to directed graphs, we consider a double marginal optimal transport problem. We study some implications of our definition and then take a closer look at hypergraphs of constant Ricci curvature. In [12, 36, 37], our notion of Ricci curvature for hypergraphs is systematically applied to empirical networks, leading to insight not readily available through other methods of network analysis. Specifically, we see that combination of the measures that we have developed, can reveal the fundamental structural properties of specific reactions as well as complex connectivity patterns in variety of real networks such as binary protein interaction networks, transcriptional regulatory networks and metabolic networks. Finally, we show that our developed geometric notions can nicely detect deviation of real networks from random models and in particular those which are obtained by shuffling the hyperedges of our real network.

5

Ollivier Ricci curvature of directed hypergraphs

In this chapter, after reviewing some basics about Riemannian-Ricci curvature as well as Ollivier's definition for graphs, we propose an Ollivier type Ricci curvature for directed hypergraphs and explore some of its properties. In particular, we will see this curvature notion can be used to characterize various classes of directed hypergraphs [13].

5.1 Preliminaries

Ricci curvature

In order to proceed, we first need to explain the geometric meaning of Ricci curvature. Ricci curvature is a fundamental concept from Riemannian Geometry (see for instance [32]) that more recently has been extended to a discrete setting. For a Riemannian manifold M of dimension N, Ricci curvature can be defined in several equivalent ways. What is relevant for the extension to the discrete setting is that it measures the local amount of non-flatness of the manifold by comparing the distance between two small balls with the distance of their centers when these centers are sufficiently close to each other. To be more precise, consider a unit tangent vector w at a point x in a Riemannian manifold M and let $\varepsilon,\ \delta > 0$ be smaller than the injectivity radius of M. Suppose $\exp_x(.) : T_x M \longrightarrow M$ denotes the exponential map and y is the endpoint of $\exp_x \delta w$ and hence at distance δ from x. Let S_x be the sphere of radius ε in the tangent space at x (and hence $\exp_x S_x$ is the sphere of radius ε around x in the manifold). Then if S_x is mapped to S_y using parallel transport, the average distance between a point of $\exp_x S_x$ and its image in $\exp_y S_y$ is

Figure 5.1

$$\delta \left(1 - \frac{\varepsilon^2}{2N}\text{Ric}\,(w,w) + O(\varepsilon^3 + \varepsilon^2\delta) \right)$$

43
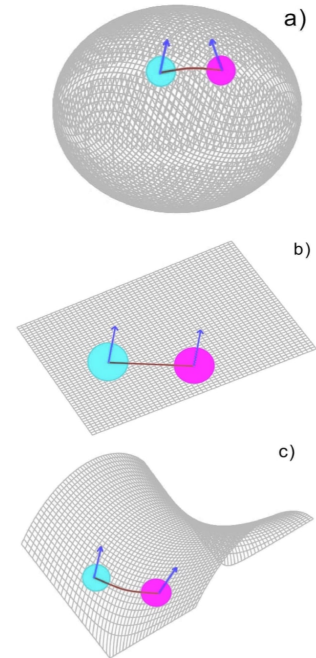
when $(\varepsilon, \delta) \to 0$. If balls are used instead of spheres, the scaling factor is $\frac{\varepsilon^2}{2(N+2)}$ instead of $\frac{\varepsilon^2}{2N}$[46]. This follows from standard Jacobi field estimates. These estimates involve the sectional curvature, but summing over all directions orthogonal to the geodesic connecting x and y results in a Ricci curvature term. Here, one should think of ε as being smaller than δ, and $O(\varepsilon^3)$ then simply indicates a higher term, whereas $O(\varepsilon^2\delta)$ is needed when the Ricci curvature is not constant. In Riemannian geometry, one can then average the Ricci curvatures of the directions at a point. This then yields the scalar curvature, which thus is a quantity naturally associated to points. The scalar curvature is a much weaker geometric invariant than the Ricci curvature. Returning to the latter, if balls in average are closer than their centers (Fig5.1, a), Ricci curvature in the direction of xy is positive. If the manifold is locally flat, Euclidian (Fig5.1, b), then the two distances coincide. Most manifolds, however, are locally negatively curved (Fig5.1, c)[41].

This local characterization is the key property for defining Ricci curvature notions in more general settings than smooth manifolds. In 2007, Ollivier defined a notion of Ricci curvature, called Ollivier (coarse) Ricci curvature, on metric spaces equipped with a random walk m; Recall that if (X, d) is a Polish metric space equipped with its Borel σ-algebra, a random walk m on X is a family of probability measures $\{m_x | x \in X\}$ satisfying the following conditions ([45]):

- The map $x \to m_x$ is measurable.

- Each m_x has finite first moment, i.e., for some (hence any) $z \in X$ one has $\int d(z, y) dm_x(y) < \infty$.

Also in the following definition, we let $d(x, y)$ be the distance from x to y obtained from the metric.

Definition 5.1.1. *[45] Let (X, d) be a metric space with a random walk m, let $x, y \in X$ be two distinct points. The Ricci curvature of (X, d, m) in the direction (x, y) is*

$$\kappa(x, y) := 1 - \frac{W_1(m_x, m_y)}{d(x, y)}$$

where W_1 is the 1-Wasserstein distance between m_x and m_y on X:

$$W_1(m_x, m_y) := \inf_{\mathcal{E} \in \Pi(m_x, m_y)} \int_{(x,y) \in X \times X} d(x, y) \mathrm{d}\mathcal{E}(x, y)$$

where $\Pi(m_x, m_y)$ is the set of measures on $X \times X$ whose first (second) marginal is m_x (m_y) (thus, each $\mathcal{E}(x, y)$ is a coupling between random walks projecting to m_x and m_y) and their support are finite discrete sets. Thus each coupling between m_x and m_y can be represented by a matrix and fining the optimal coupling is done by solving a linear programming.

Here instead of taking metric balls around two close enough points we consider the Wasserstein distance (Transportation or Earthmover distance), between two probability

measures m_x and m_y corresponding to two random walks which are starting at x and y respectively. When (X, d, m) is Riemannian manifold equipped with Riemannian volume measure, as it is shown in [45], this notion coincides with the Riemannian Ricci curvature in the direction of xy (up to some scaling factor).

In 2010 Lin et.al modified Ollivier's definition on graphs to study the properties of the Ricci curvature of general graphs. Specifically they presented some bounds for this curvature on locally finite graphs and established the upper bounds for diameters and the number of vertices in terms of Ollivier-Ricci curvature on graphs [39]. For a (locally finite) graph, the two measures m_x and m_y are discrete and their supports are finite. Namely for two input (discrete) distributions on the graph we have:

$$m_x = \sum_{i=1}^{n} a_i \delta_{x_i} \qquad m_y = \sum_{j=1}^{m} b_j \delta_{y_j}$$

and since the graph is locally finite, there are finite points in the support of these measures :
$(x_i)_{1 \leq i \leq n}$, $(y_j)_{1 \leq j \leq m}$
where each of these points might get different weights:
$a_i \geq 0$, $b_j \geq 0$.

$$\sum_{i=1}^{n} a_i = \sum_{j=1}^{m} b_j = 1$$

Thus a coupling can be represented as the following matrix:

$$\mathcal{E}(m_x, m_y) \overset{\text{def}}{=} \{C \in \mathbb{R}_+^{n \times m} : C \mathbb{1}_n = m_x, C^T \mathbb{1}_m = m_y\}$$

As an example, consider the green edge in following graph; this edge is a connection between vertices x in the left and y in the right and we have two measures, coloured respectively by red and blue, which are defined based on randomly jumping from x and y to their adjacent vertices.
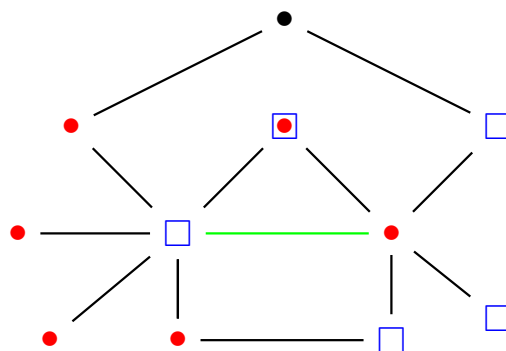

Figure 5.2

Here we consider unweighed graphs and as x has six adjacent vertices, each $a_i = 1/6$ and similarly each $b_j = 1/5$ since y has five adjacent vertices. Therefore $\mathcal{E}(x_i, y_j)$ is the amount

of mass that is moved from red square in x_i to fill the blue hole in y_j.

Liu and Jost [33] interpreted the notion of Ricci curvature of an edge as a control on the amount of overlap between the neighborhoods of its involving vertices and obtained curvature bounds on graphs in terms of local clustering coefficients, which is defined based on the presence of triangles containing those vertices. More recently, in [1], the notion of Ollivier-Ricci curvature was naturally extended to undirected hypergraphs. Recall that an undirected hypergraph $H = (V, E)$ consists of a set V of vertices and a multiset E of subsets of V, called hyperedges ($\forall e \in E, |e| \leq |V|$). Therefore, as a generalization of edges in graphs which connect two vertices, hyperedges represent connections between any number of vertices. In [1], this leads to

Definition 5.1.2. *Coarse Scalar Curvature For a collection of n points $X_n := \{x_1, \ldots, x_n\}$ in a metric space (X, d) with random walk $m := \{m_x | x \in X\}$, coarse scalar curvature of X_n is defined as:*

$$\kappa(X_n) := 1 - \frac{W_1(X_n)}{c(x_1, x_2, \ldots, x_n)}$$

$$W_1(X_n) = \inf_{\nu \in \Pi(m_x, \nu)} \sum W_1(m_x, \nu)$$

$$c(x_1, \ldots, x_n) = \inf_{z \in X} \sum_{i=1}^{n} d_X(x_i, z)$$

If $\{x_1, \ldots, x_n\}$ are the vertices of a hypergraph connected by a hyperedge e, then the above formula for scalar curvature is an extension for the edge Ricci curvature in an undirected graph[33] (when $n = 2$ in every hyperedge).

In network analysis, and particularly for networks that are modelled as undirected graphs, Ollivier Ricci curvature has proved itself as a very useful tool to determine clustering and coherence in the network [33, 50], and since it is based on Markov chains, it is very well suited for capturing diffusion and stochastic processes in the network. One can see this as a motivation for the above definition of [1] on undirected hypergraphs, where multi-marginal optimal transport was used. Since this is defined for points rather than for directions, from our perspective, this should be considered as a version of scalar curvature, rather than of Ricci curvature. However, the definition we shall present in the next section will be different. Before going to our main formulation and results on Ollivier Ricci curvature of directed hypergraphs, we need to be more familiar with the structure of directed graphs and some of the main approaches that have been taken in the literature for defining some of analytical and geometrical notions such as Laplacian and curvature on these settings.

Directed graphs are more difficult to analyse than undirected graphs as we do not have a unique notion for some of the most basic definitions. For instance although we have a unique and straightforward notion of connectedness in undirected (hyper) graphs, we have two main connectivity notions for the directed setting, weakly-connectedness and strongly-

connectedness; we call a directed (hyper)graph weakly-connected if the underlying directed (hyper) graph is connected, namely there is a path between every two vertex of hypergraph. On the other side, when there is a directed path between any vertex of directed (hyper) graph to any other, it is strongly connected. Thus strongly-connectedness is much more restricted than weakly-connectedness as every strongly-connected directed (hyper)graph is weakly-connected but to make a strongly-connected directed (hyper)graph from a weakly-connected one we might need to add so many directed (hyper)edges between the existing vertices. Subsequently, there are two main approaches in the literature for defining Laplacian and curvature notions for directed graphs; in the first approach we consider strongly- connected directed graphs. Additionally assigned weights to directed edges are all non-negative. In the contrary, in the second approach neither of these two assumptions have been assumed. Each of these approaches has its own bountiful advantages; the first approach implicates that the Perron measure (stationary distribution of Markov chain) exists and consequently we can define a type of symmetric and non-negative Laplacian [8]. Also many of analytical or geometrical results can be extended to the directed settings with proofs similar to their undirected counterparts [47].

In the second approach however, as its presented by Bauer [5] for defining Laplacian notions, the main motivation is dealing with real-word structures and developing some tools which are useful for the analysis of complex networks. Developing such tools, is crucial since many real networks, such as neural networks or chemical reaction networks, are far from being strongly-connected. On the other side, cyclic graphs, which for instance are important for inferring causality relation, are not strongly connected. This approach is what we consider in the next section to define Olliver-Ricci curvature of directed hypergraphs.

5.2 Transport plans and curvature of directed hypergraphs

As already mentioned, similar to directed graphs, in directed hypergraphs, every hyperedge e in E represents a directional relation between two non-empty subsets A_e (tail), B_e (head) of the vertex set V. In this chapter we often write A instead of A_e, and B instead of B_e when the hyperedge e is specified and fixed. Note that the sets A_e, B_e and V can be equal, namely when the hypergraph has just one hyperedge e and its tail set and head set coincide. However if for a hyperedge e, A_e or B_e is a proper subset of V, then since we consider non-empty subsets of V, the other one should also be proper. Similarly, for any vertex $x \in V$, d_x^{in} is the number of incoming hyperedges to x (those hyperedges which include x in their head set), and d_x^{out} is the number of outgoing hyperedges from x (those hyperedges which have x in their tail set). Also a directed path between the vertices in a directed hypergraph G is an alternating sequence of distinct vertices and directed hyperedges $(v_1, e_1, ..., v_k, e_k, v_{k+1})$ such that for each i, v_i and v_{i+1} are in the tail and head sets of e_i respectively. If $k \geq 1$ and v_1 and v_{k+1} are the same vertices, the path is called a directed k-cycle. From now

on we consider directed hypergraphs to be weakly connected, meaning that the underling undirected hypergraph is connected.

Definition 5.2.1. *Let $H = (V, E)$ be an unweighted directed hypergraph and $e \in E$ be an arbitrary directed hyperedge such that $A = \{x_1, \ldots, x_n\} \overset{e}{\to} B = \{y_1, \ldots, y_m\}$ $(n, m \leq |V|)$. We define the Ollivier Ricci curvature of this hyperedge as*

$$\kappa(e) := 1 - W(\mu_{A^{in}}, \mu_{B^{out}})$$

where the probability measures $\mu_{A^{in}}$ (called mass) and $\mu_{B^{out}}$(called hole), are defined on V as follows:

$\mu_{A^{in}} = \sum_{i=1}^{n} \mu_{x_i}^{in}$ *where* $\forall 1 \leq i \leq n$ *and* $\forall z \in V(H)$

$$\mu_{x_i}^{in}(z) = \begin{cases} 0 & z = x_i \ \& \ d_{x_i}^{in} \neq 0 \\ \frac{1}{n} & z = x_i \ \& \ d_{x_i}^{in} = 0 \\ \displaystyle\sum_{e'; x_i \in B_{e'}, \ z \in A_{e'}} \frac{1}{n \times d_{x_i}^{in} \times |A_{e'}|} & z \neq x_i \ \& \ z \in A_{e'} \\ 0 & \text{otherwise} \end{cases}$$

and likewise

$\mu_{B^{out}} = \sum_{j=1}^{m} \mu_{y_j}^{out}$ *where* $\forall 1 \leq j \leq m, z \in V(H)$:

$$\mu_{y_j}^{out}(z) = \begin{cases} 0 & z = y_j \ \& \ d_{y_j}^{out} \neq 0 \\ \frac{1}{m} & z = y_j \ \& \ d_{y_j}^{out} = 0 \\ \displaystyle\sum_{e'; y_j \in A_{e'}, \ z \in B_{e'}} \frac{1}{m \times d_{y_j}^{out} \times |B_{e'}|} & z \neq y_j \ \& \ z \in B_{e'} \\ 0 & \text{otherwise} \end{cases}$$

and $W(\mu_{A^{in}}, \mu_{B^{out}})$ is the 1-Wasserstein distance between these two discrete measures defined as follows:

$$W(\mu_{A^{in}}, \mu_{B^{out}}) = \min_{\mathcal{E} \in \Pi(\mu_{A^{in}}, \mu_{B^{out}})} \sum_{u \to A} \sum_{B \to v} d(u, v)\mathcal{E}(u, v)$$

where $d(u, v)$ is the length of a shortest path from u to v and for a transport plan $\mathcal{E}$, $\mathcal{E}(u, v)$ represents the amount of mass moved from vertex u to vertex v and $\Pi(\mu_{A^{in}}, \mu_{B^{out}})$ is the set of transport plans, that is, probability measures on $V \times V$ that have $\mu_{A^{in}}$ and $\mu_{B^{out}}$ as their marginals. In other words, the minimum is taken over all couplings $\mathcal{E}$ between $\mu_{A^{in}}$ and $\mu_{B^{out}}$ which satisfy

$$\sum_{u \to A} \mathcal{E}(u, v) = \sum_{j=1}^{m} \mu_{y_j}^{out}(v) \ \text{and} \ \sum_{B \to v} \mathcal{E}(u, v) = \sum_{i=1}^{n} \mu_{x_i}^{in}(u)$$

and by $A^{in}(u \to A)$ we mean the vertices $u \in V$ with $\mu_{A^{in}}(u) \neq 0$. Similarly $B^{out}(B \to v)$ refers to the vertices $v \in V$ with $\mu_{B^{out}}(v) \neq 0$.

Remark 5.2.2. *Since we are working with directed objects, in this definition we had to provide for the situation where a vertex in the tail does not have incoming connections, or where a vertex in the head does not have any outgoing ones. In undirected networks, this is not an issue, because then the hyperedge in question itself provides both.*

We can construct for each directed hypergraph a corresponding directed graph. That graph has the same set of vertices as the directed hypergraph and for each hyperedge, we draw an edge from each vertex in its tail to every vertex in its head. Thus, a directed hyperedge $A = \{x_1, \ldots, x_n\} \xrightarrow{e} B = \{y_1, \ldots, y_m\}$ corresponds to a set with nm elements of directed edges. Note, however, that there might be directed graphs that correspond to more than one directed hypergraph.

Proposition 5.2.3. *The curvature of a hyperedge $e : A = \{x_1, \ldots, x_n\} \rightarrow B = \{y_1, \ldots, y_m\}$ is bounded from below by the minimum of the Ricci curvatures of directed edges in its corresponding directed graph.*

Proof. Let $\mathcal{E}_{ij}$ be the optimal transport plan for the edge $e_{ij} : x_i \rightarrow y_j$, i.e.

$$W(\mu_{x_i}^{in}, \mu_{y_j}^{out}) = \sum_{u,v \in V} d(u,v) \mathcal{E}_{ij}(u,v)$$

Then

$$\mathcal{E} := \frac{1}{mn} \sum_{i=1}^{n} \sum_{j=1}^{m} \mathcal{E}_{ij}$$

has the marginal distributions $\mu_{A^{in}}$ and $\mu_{B^{out}}$. Therefore :

$$W(\mu_{A^{in}}, \mu_{B^{out}}) \leq \sum_{u,v \in V} d(u,v) \mathcal{E}(u,v) = \frac{1}{mn} \sum_{i=1}^{n} \sum_{j=1}^{m} W(\mu_{x_i}^{in}, \mu_{y_j}^{out}) \leq \max_{\substack{1 \leq i \leq n \\ 1 \leq j \leq m}} W(\mu_{x_i}^{in}, \mu_{y_j}^{out})$$

and therefore $\kappa(e) \geq \min_{\substack{1 \leq i \leq n \\ 1 \leq j \leq m}} \kappa(e_{ij})$. $\qquad \square$

However, the corresponding directed edges of a directed hyperedge do not fully represent the geometric structure of that hyperedge as shown in the following

Remark 5.2.4. *The maximum of the Ricci curvatures of directed edges corresponding to a directed hyperedge is not necessarily an upper bound for its Ricci curvature, as one can see from the example where the curvature of the hyperedge with red colour is one and the curvature of all its four corresponding directed edges is $-1/2$.*
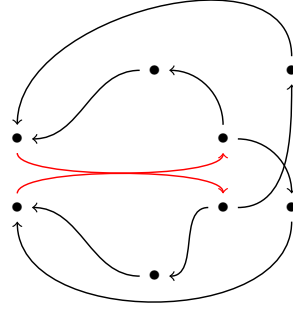
Figure 5.3

Lemma 5.2.5. *For a directed hyperedge $e : A \to B$ we have*

$$W(\mu_{A^{in}}, \mu_{B^{out}}) \geq \sup \left(\sum_{u \to A} f(u)\mu_{A^{in}}(u) - \sum_{B \to v} f(v)\mu_{B^{out}}(v) \right)$$

where the supremum is taken over all functions on $V(H)$ with $f(u) - f(v) \leq d(u,v)$.

Proof. The proof is similar to the proof of proposition 2.10 in [57] where another measure (out-out) for defining Ricci curvature of a directed edge is considered. Here we show that the same result holds for directed hypergraphs by assuming other directions (in-out) for defining measures. We have :

$$\sum_{u \to A} \sum_{B \to v} d(u,v)\mathcal{E}(u,v) \geq \sum_{u \to A} \sum_{B \to v} (f(u) - f(v))\mathcal{E}(u,v)$$

$$= \sum_{u \to A} f(u) \sum_{B \to v} \mathcal{E}(u,v) - \sum_{B \to v} f(v) \sum_{u \to A} \mathcal{E}(u,v)$$

thus:

$$= \sum_{u \to A} f(u)\mu_{A^{in}}(u) - \sum_{B \to v} f(v)\mu_{B^{out}}(v)$$

and since for all Lipschitz functions on hypergraphs this inequality holds and the left hand side is independent of f, we obtain

$$W(\mu_{A^{in}}, \mu_{B^{out}}) \geq \sup \left(\sum_{u \to A} f(u)\mu_{A^{in}}(u) - \sum_{B \to v} f(v)\mu_{B^{out}}(v) \right).$$

$\square$

Remark 5.2.6. *In general, we do not get equality in this lemma; equality holds for undirected hypergraphs (see [57]), or more generally, if for every directed hyperedge e from A_e to B_e, we have a directed hyperedge e' in the reverse direction, from B_e to A_e (i.e, $A_{e'} = B_e$, $B_{e'} = A_e$). In that case, all distances $d(u,v)$ become symmetric.*

We now propose another formula for the curvature of a hyperedge which is more intuitive and in some cases much easier to work with.

For defining the Ricci curvature of a hyperedge e, we use incoming hyperedges to its tail set (A_e) and outgoing hyperedges from its head set (B_e). If u and v are in the support of $\mu_{A^{in}}$ and $\mu_{B^{out}}$ respectively, then $d(u, v) \leq 3$. Recall that for any real valued function f on V, the support of f (denoted by $supp f$) is the set of all vertices in V where f is non-zero, i.e., $supp(f) = \{u \in V \mid f(u) \neq 0\}$.

If μ_i is the amount of mass that is moved with distance $i (i \leq 3)$ in an optimal transport plan, then we have:

$$\sum_{i=0}^{3} \mu_i = 1, \; \sum_{i=1}^{3} i\mu_i = W. \tag{5.1}$$

If $\kappa = 0$ then $W = 1$, and we thus have $\mu_0 = \mu_2 + 2\mu_3$. More generally, we obtain

Theorem 5.2.7. *The curvature of a hyperedge is given by*

$$\kappa = \mu_0 - \mu_2 - 2\mu_3. \tag{5.2}$$

In fact, we could simply use (5.2) as a *definition* of Ricci curvature. The formula (5.2) for the curvature of a directed hyperedge, also works for curvature of edges in undirected graphs. As in the (undirected) graph case, μ_0 represents the amount of mass which is not moved in an optimal plan, i.e., the amount of the stable mass in directed 3-cycles ($u \to x_i \to y_j \to u$) (where u is simultaneously in the support of $\mu_{A^{in}}$ and $\mu_{B^{out}}$) or directed loops emerging from any of the x_is. Although μ_1 (the mass moved with distance one, possibly through directed quadrangles ($u \to x_i \to y_j \to v$, while u is directly connected to v, $u \to v$) does not appear in the formula for the curvature, computing μ_1 is an intermediate step for the computations of μ_2 and μ_3 where μ_2 is the amount of mass that should be moved with distance 2 (possibly through directed pentagons including x_i and y_j) and μ_3 is the amount of the mass that is moved with distance 3 in an optimal plan.

Remark 5.2.8. *While finding the general formula for μ_1 (and μ_2) may be difficult, any lower bound for μ_1 (after simply knowing the exact amount of μ_0) helps us to derive some upper bounds for W and therefore a lower bound for the curvature. Also the μ_i can differ between different optimal transport plans, but equalities (5.1) and (5.2) will always hold.*
We also point out that while optimal transport plans always exist in our finite setting, they need not be unique.

Remark 5.2.9. *Formula* (5.2) *for edges in undirected graphs simply implicates that:*

  i) *κ is bounded above by 1 and from below by -2.*

  ii) *we can relate the local shape of graphs with the presence of triangles, quadrangles and pentagons.*

iii) By averaging over all Ricci curvatures of the edges connected to a point, we get a type of scalar curvature at that point which is controlled by the local clustering coefficient [33].

As an example, in the following figure, for computing the curvature of the green hyperedge which connects 3 vertices in its left(A) to 2 vertices in its right(B), separated by dots, we assign masses (red bullets) and holes (empty squares) respectively to the incoming neighbours of A and outgoing neighbours of B. Note that since for a vertex x in A (the lowest vertex in A), $d_x^{in} = 0$, we put all its assigned mass at x which is equal to $1/3$. Similarly there is a vertex y in B such that $d_y^{out} = 0$. Therefore we put its whole assigned measure at y itself and it is equal to $1/2$. Also for the other vertices in A (respectively B), their assigned masses (holes) are divided between the vertices in the tails of incoming hyperedges to A (the vertices in the heads of outgoing hyperedges from B) based on Definition 5.2.1. It is straightforward to check that in (any) optimal transport plan, $1/12$ of the mass need not be moved. This is the amount of the mass which coincides with one of the holes. Also $1/3$ of the mass at x is moved with distance one to the hole at y. $1/6$ is moved with distance two and the remained part is moved with distance three. Hence the curvature of the green hyperedge is $-11/12$.
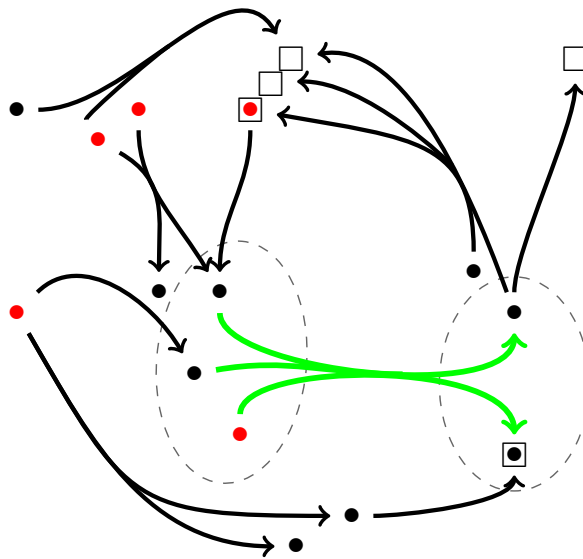

Figure 5.4

Bounds for the curvature

For obtaining an upper bound for the curvature of a hyperedge we need to control μ_0 which corresponds to the stable mass at directed 3 cycles (triangles in the undirected graph case) and those vertices which are in the intersection of A and B.

In what follows, we shall see that increasing the number of vertices in this intersection will make the curvature more positive. Here, a directed hyperloop is a directed hyperedge $e : A = \{x_1, \ldots, x_n\} \to B = \{y_1, \ldots, y_m\}$ for which $A \cap B$ is non-empty. Specifically

where $A \cap B = A = B$, we shall have $\kappa(e) = 1$. Directed k-cycles where $k \geq 4$ do not affect the curvature of directed hyperedges since they can not make short-cuts for moving any of the masses to any of the holes.

Proposition 5.2.10. *For a directed hyperedge $e : A = \{x_1, \ldots, x_n\} \to B = \{y_1, \ldots, y_m\}$ we have*

$$\sum_{u \in \text{supp } \mu_{A^{in}}(u) \cup \text{supp } \mu_{B^{out}}} \mu_{A^{in}}(u) \wedge \mu_{B^{out}}(u) \geq \kappa(e).$$

Where $\alpha \wedge \beta := min\{\alpha, \beta\}$.

Proof. Jost and Liu have established this theorem in undirected graphs (thorem 7 in [33]). Here, we simply notice that the number of non-zero elements in this summation coincides with the number of vertices u belonging to a directed 3-cycle $(u \to x_i \to y_j \to u)$ or $A \cap B$. For other vertices u either of $\mu_{A^{in}}(u)$ or $\mu_{B^{out}}(u)$ is zero.

Also the equality holds when for a hyperedge e, all the masses coincide with all the holes with the same size. For instance in isolated directed hyperloops when $A \cap B = A = B$ both sides of the above formula are equal to one. As another general example see Lemma 5.2.22. $\square$

As already mentioned in Remark 5.2.8 after computing μ_0, any non-zero amount for μ_1 would give us an upper bound for W. For that, at least one incoming neighbour of A should be at distance one from some outgoing neighbour of B. For example, when for the hyperedge e, $e : A = \{x_1, \ldots, x_n\} \to B = \{y_1, \ldots, y_m\}$, there is at least one hyperedge e' from any y_j to any x_i ($e' : y_j \to x_i$) or/ and when there is at least one x_i with $d_{x_i}^{in} = 0$ and at least one y_j with $d_{y_j}^{out} = 0$, the required condition is sattisfied and there is at least one mass which is in distance one from at least one hole and therefore we can present a transfer plan (similar to that in Theorem 3 in [33]) to obtain a positive lower bound for μ_1. Specifically, in the same way that trees reach the smallest possible amount of curvature in undirected graphs, here hyperedges in directed hypertrees get the lowest possible number.

Definition 5.2.11. *A directed loopless hypergraph is a hypertree if*

  i) *There is at most one directed path between any two vertices and*

  ii) *It does not contain any directed cycle.*

We note that although these two conditions are equivalent in undirected (hyper)graphs, they do not coincide in the directed case.

Theorem 5.2.12. *Let $A = \{x_1, \ldots, x_n\}$ and $B = \{y_1, \ldots, y_m\}$ be two subsets of vertices V of a hypertree H with respectively n and m elements and $A \xrightarrow{e} B$ be a hyperedge in this hypertree. If k elements in A have no incoming hyperedge, namely $\#\{x_i \in A, d_{x_i}^{in} = 0\} = k$ and k' element in B have no outgoing hyperedge, i.e $\#\{y_j \in B, d_{y_j}^{out} = 0\} = k'$, we have :*
$\kappa(e) = -2 + \frac{k}{n} + \frac{k'}{m}.$

Proof. Note that since e is in a hypertree, according to the definition $\mu_0 = 0$. Hence in a hypertree, the curvature of any hyperedge is non-positive ($\kappa(e) \leq 0$). We shall propose a transfer plan, which gives us an upper bound for W, and we will obtain a lower bound for W based on a single Lipschitz function (defined on the support of $\mu_{A^{in}}$ and $\mu_{B^{out}}$). We shall see that these two bounds coincide.

First we move $(\frac{k}{n} \wedge \frac{k'}{m})$ of the mass from k x_i's to k' y_j's with distance one. Then if $\frac{k}{n} \geq \frac{k'}{m}$ we move $\frac{k}{n} - \frac{k'}{m}$ of the mass from x_i's with no incoming hyperedges to outgoing neighbours of the y_j's with distance 2 and if $\frac{k'}{m} > \frac{k}{n}$ we move $\frac{k'}{m} - \frac{k}{n}$ of the mass at incoming neighbours of x_i's to those y_j's with no outgoing hyperedges with distance 2. Then we move the remaining part of the mass with distant 3. Therefore $W \leq 3 - \frac{k}{n} - \frac{k'}{m}$.

On the other hand, for all z in $V(H)$ we define

$$f(z) = \begin{cases} 3 & \exists 1 \leq i \leq n \& \exists e : z \to x_i \\ 2 & \exists 1 \leq i \leq n \& z = x_i \\ 1 & \exists 1 \leq j \leq m \& z = y_j \\ 0 & \text{otherwise} \end{cases}$$

It is straightforward to check that f is a Lipschitz function on $A \cup B \cup \text{supp}\mu_{A^{in}} \cup \text{supp}\mu_{B^{out}}$, hence according to the theorem 3.5, we have

$$\begin{aligned} W(\mu_{A^{in}}, \mu_{B^{out}}) &\geq \sup \sum_{z \to A} \mu_{A^{in}}(z)f(z) - \sum_{B \to z'} \mu_{B^{out}}(z')f(z') \\ &\geq 3\left(1 - \frac{k}{n}\right) + 2\left(\frac{k}{n}\right) - 1 \times \frac{k'}{m} - 0 \times \left(1 - \frac{k'}{m}\right) \\ &= 3 - \frac{k}{n} - \frac{k'}{m}. \end{aligned}$$

and $\kappa(e) = -2 + \dfrac{k}{n} + \dfrac{k'}{m}$. $\qquad \square$

Proposition 5.2.13. *If for all $1 \leq i \leq n$, $1 \leq j \leq m$, $d_{x_i^{in}} \neq 0$ and $d_{y_j^{out}} \neq 0$ and there is a bijective map $g : \text{supp } \mu_{A^{in}} \to \text{supp } \mu_{B^{out}}$ such that $g(z) = z'$ and $d(z, z') = 1$ and $\mu_{A^{in}}(z) = \mu_{B^{out}}(z')$ then $\kappa(e) = 0$.*

Proof. By assumption, $\mu_0 = 0$ and the whole mass in any transport plan has to be moved with distance at least one. Also we know that the bigger μ_1, the lower the cost of the transport between $\mu_{A^{in}}$ and $\mu_{B^{out}}$. But according to the assumption there is a direct (length 1) path between every pair (z, z') and it's corresponding hole at z' can be filled with mass at z (no further mass remains at z). Therefore $\mu_1 = 1$, $W = 1$ and $\kappa = 0$ $\qquad \square$

Remark 5.2.14. *In the above proposition, neither of the assumptions is necessary to have $\kappa = 0$. In such cases a more subtle transfer plan is needed. For instance in the following*
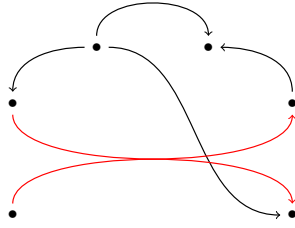
hypergraphs, the red hyperedge has curvature zero.

Remark 5.2.15. *With the same assumptions as in the previous theorem, but changing the assumption $d(z, z') = 1$ to $d(z, z') = 2$ and assuming there is no directed quadrangle $(u \to x_i \to y_j \to v, u \to v)$, the curvature will become negative (-1). Since in this case the distance between any mass and it's corresponding hole is 2 and no hole can be filled with a mass at lower distance.*

Extention and Reduction

- **Removing vertices from a hyperedge (Reduction)** In this part we want to investigate what happens to the curvature of an edge $e : A = \{x_1, \ldots, x_n\} \to B = \{y_1, \ldots, y_m\}$ if we remove a number (l, l') of vertices from A $(l \leq n)$ and/or from B $(l' \leq m)$. Curvature depends on the connections between elements of $\operatorname{supp} \mu_{A^{in}}$ and $\operatorname{supp} \mu_{B^{out}}$ and removing different vertices from $A(and/or B)$ might have different effects on the curvature. However since the amount of the masses (size of holes) which is assigned to any x_i(and y_j) is already determined and is equal to respectively $1/n$ (and $1/m$), we can give a bound for such changes.

Proposition 5.2.16. *Let $e : A = \{x_1, \ldots, x_n\} \to B = \{y_1, \ldots, y_m\}$. By removing a vertex x_i from A we get $e' : A - \{x_i\} \to B = \{y_1, \ldots, y_m\}$ and we have*

$$|\kappa(e') - \kappa(e)| \leq \frac{3}{n}.$$

Similarly, by removing l vertices from A $(l < n)$ we have

$$|\kappa(e') - \kappa(e)| \leq \frac{3l}{n}$$

Proof. The two bounds for the curvature of e' arise from two extreme scenarios which might happen while removing vertex x_i (or l vertices) from A.

1. If the whole mass which is assigned to x_i is in directed loops or directed 3-cycles including x_i and any of y_j s, and after removing x_i, its corresponding mass has to be moved with distance 3 in an optimal plan, then

$$\begin{cases} \kappa(e) = \mu_0 - \mu_2 - 2\mu_3 \\ \kappa(e') = \left(\mu_0 - \dfrac{1}{n}\right) - \mu_2 - 2\left(\mu_3 + \dfrac{1}{n}\right). \end{cases}$$

2. If the whole mass around x_i was transported with distance 3 in an optimal plan and after removing this vertex, the corresponding mass is in the place of directed loops or directed 3-cycles including vertices of $A - \{x_i\}$ and B, then

$$\kappa(e') = \left(\mu_0 + \frac{1}{n}\right) - \mu_2 - 2\left(\mu_3 - \frac{1}{n}\right) = \kappa(e) + \frac{3}{n}.$$

Therefore we have

$$\kappa(e) + \frac{3}{n} \geq \kappa(e') \geq \kappa(e) - \frac{3}{n}.$$

The same argument works for removing l vertices from A and the proof is complete.

□

Analogously, by removing l' vertices from B ($l' < m$) and using the same argument as before for the holes assigned to B, we have

$$|\kappa(e') - \kappa(e)| \leq \frac{3l'}{m}.$$

Therefore :

Proposition 5.2.17. *By removing l vertices from the set A and l' vertices from B ($e : A \rightarrow B$) the following relation holds between the curvature of the resulting hyperedge (e') and the old one :*

$$|\kappa(e') - \kappa(e)| \leq 3\left(\frac{l}{n} + \frac{l'}{m}\right) \wedge 3$$

- **Adding vertices to a hyperedge (Extension)** Here we want to obtain bounds for the curvature of a hyperedge obtained by adding some new vertices to the set A and/or to B and possibly adding new connections between them.

Proposition 5.2.18. *Let $e : A = \{x_1, \ldots, x_n\} \rightarrow B = \{y_1, \ldots, y_m\}$. By adding l vertices to A and l' vertices to B we get a hyperedge $e' : A' = \{x_1, \ldots, x_{n+l}\} \rightarrow B' = \{y_1, \ldots, y_{m+l'}\}$ with*

$$|\kappa(e') - \kappa(e)| \leq 3\left(\frac{l}{l+n} + \frac{l'}{l'+m}\right) \wedge 3$$

Proof. Here, since to each x_i in A' we assign $\frac{1}{l+n}$ of the total mass ($= 1$) and $\frac{1}{l'+m}$ of the total hole ($= 1$) is assigned to each y_j in B', by considering the two extreme scenarios as before we have:

$$\mu_0(e) \rightarrow \mu_0(e') \pm \left(\frac{l}{l+n} + \frac{l'}{l'+m}\right) \wedge 1$$

and therefore:

$$\mu_3(e) \to \mu_3(e') \mp \left(\frac{l}{l+n} + \frac{l'}{l'+m} \right) \wedge 1$$

and according to the formula 5.2 the proof is complete. $\qquad\qquad\square$

Hypergraphs with constant Ricci curvature

We want to construct examples of directed hypergraphs in which the curvature of the hyperedges is constant ($\kappa = 1, \kappa = 0, \kappa = -2$). In the case of $\kappa = 0$ these (hyper)graphs are called Ricci flat. For brevity, we also call the others Ricci 1 and Ricci -2 directed hypergraphs.

- **Ricci 1 directed hypergraphs**

Theorem 5.2.19. *The vertices of a Ricci 1 directed loopless hypergraph which for every hyperedge $e : \{x_1, \ldots, x_n\} \to \{y_1, \ldots, y_m\}$ does not have any hyperedge in the reverse direction ($\nexists e' : y_j \to x_i$), can be divided into 3 subsets A, B, C such that $A \to B \to C \to A$. This means that some (not necessarily all) vertices in A are connected to vertices in B via a non-empty collection of directed hyperedges and similarly for the other connections as in the following diagram.*
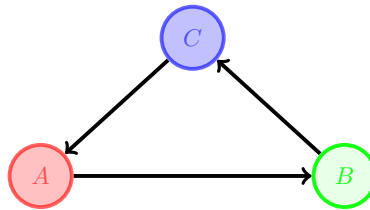
Figure 5.6

Proof. Consider a hyperedge $e_1 : A_1 \to B_1$. Since $\kappa(e_1) = 1$

$$\operatorname{supp} \mu_{A_1^{in}} = \operatorname{supp} \mu_{B_1^{out}} =: C_1 \quad \text{and} \quad \forall z \in C_1 : \mu_{A_1^{in}}(z) = \mu_{B_1^{out}}(z) \qquad (5.3)$$

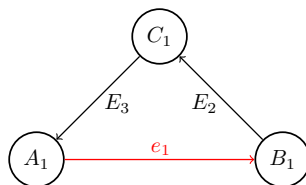So the diagram related to e_1 looks like

Figure 5.7

where E_2 and E_3 represent collections of directed hyperedges. Now, if there is no outgoing hyperedge from C_1 other than elements in E_3 and there is no incoming hyperedge to C_1 other than elements of E_2 and there is no outgoing hyperedge other

than e_1 from A_1 and there is no incoming hyperedge to B_1 other than e_1, then A_1, B_1 and C_1 would be the desired partitioning set; Since the hypehgraph is loopless, the intersection of any two of these sets is empty and because it is weakly connected the union of the vertices is the whole vertices set, V(H). If any of the above conditions does not hold, we can extend A_1 and/or B_1 and/or C_1 as follows:

For instance, let there be at least one hyperedge going out of A_1 other than e_1; we call it $e_{OA_1} : A_1 \to B_{11}$ and we put $B_2 = B_1 \cup B_{11}$ where B_1 and B_{11} are not necessarily disjoint. Since $\kappa(e_{OA_1}) = 1$, so $C_2 := \text{supp } \mu_{B_{11}^{out}} = \text{supp } \mu_{A_1^{in}} \supseteq C_1$. We next consider edges in E_3; If any of them has an endpoint outside A_1 and if the set of endpoints of E_3 is denoted by A_2, then $A_1 \subseteq A_2$. By repeating this process we obtain an increasing sequence of A_i's, B_j's and C_k's. We put $A = \cup A_i$, $B = \cup B_j$ and $C = \cup C_k$. Obviously, based on the process, elements in A are connected to B, B to C and C to A and these 3 sets are our desired partitioning.

Figure 5.8

$\square$
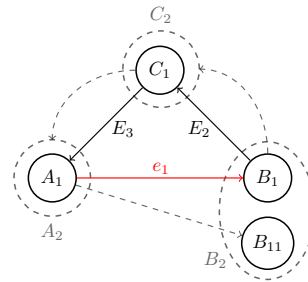
Remark 5.2.20. *The converse of this theorem is not necessarily true. For instance, the following hypergraph is not Ricci 1 although there is such a partitioning for the set of vertices of this hypergraph:*
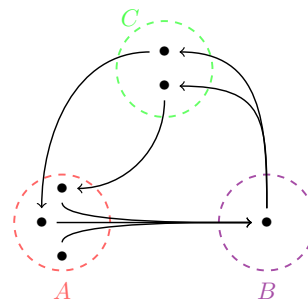

Figure 5.9

Instead we have the following:

Proposition 5.2.21. *If in the corresponding directed graph of a directed (loopless) hypergraph, the set of vertices can be partitioned into 3 different sets A, B, C such that $A \to B \to C \to A$ and all of the elements in A are connected (via directed*

edges) to all the elements in B and similarly for the other arrows as above, then the original directed hypergraph is Ricci 1.

Before proving this Proposition we state the next Lemma.

Lemma 5.2.22. *A directed (loopless) graph is Ricci 1 iff it's set of vertices can be partitioned into 3 sets A, B, C such that $A \to B \to C \to A$ and all the vertices in A are connected to all the vertices in B and similarly for the other arrows, as in the digram in previous theorem.*

Proof. $\Rightarrow$ The proof is similar to that of Theorem 5.2.19. Here, in addition all the vertices of A should be connected to all the vertices of B and so on. The reason is that here, for every edge $e : x \to y$, $d_{in}x = d_{out}y$, and the condition that $\text{supp }\mu_{x^{in}} = \text{supp }\mu_{y^{out}}$ implies that the tails of incoming edges to x coincide with the heads of outgoing edges from y. Hence in the resulted partition every vertex in A is connected to every vertex in B and similarly for the connections between other sets the same situation holds.

$\Leftarrow$ For proving that every edge has curvature 1, for every edge $e : x \to y$, we should have $d_{in}x = d_{out}y$ and $\text{supp }\mu_{x^{in}} = \text{supp }\mu_{y^{out}}$ and for every z in this support $\mu_{x^{in}}(z) = \mu_{y^{out}}(z)$. Since in the partition all the vertices in A are connected to all the vertices of B and so on, for every edge the needed conditions obviously hold and the directed graph is Ricci 1. $\qquad\square$

Proof of Proposition 5.2.21. Since we have such a partition for the vertices of the corresponding directed graph of this hypergraph, according to the previous Lemma, the curvature of all the corresponding edges of each directed hyperedge is 1. Therefore their minimum also has curvature 1. On the other hand, according to Proposition 5.2.3

$$\kappa(\text{every hyperedge}) \geq \min \kappa(\text{edges in the corresponding directed graph})$$

So for all hyperedges e, $\kappa(e) = 1$ and the hypergraph is Ricci 1. $\qquad\square$

Remark 5.2.23. *It might be possible that the directed hypergraph is Ricci 1, but as shown in the following example, its corresponding directed graph is not.*
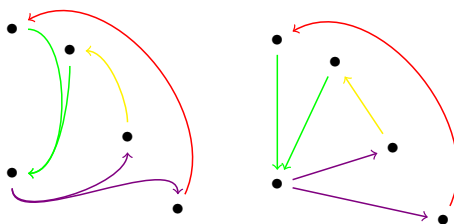

Figure 5.10

Corollary 5.2.24. *If in a directed (loopless) hypergraph, the set of vertices can be partitioned into 3 different sets A, B, C such that $A \to B \to C \to A$ and all of the elements in A are connected (via directed hyperedges) to all the elements in B and similarly for the other arrows, the directed hypergraph is Ricci 1. Here any connection inside any of these sets might violate the constant curvature 1 for some hyperedges. For instance, in the following directed graph, the curvature of all the edges is 1 but the red edge has curvature -1 .*
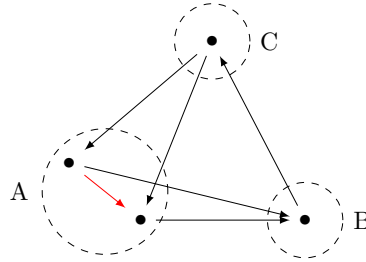
Figure 5.11

• **Ricci flat directed hypergraphs**

Theorem 5.2.25. *If the vertices of a directed hypergraph can be divided, as in the left diagram, into two sets A (source) and B (sink) such that all the vertices in A have outgoing hyperedges and no incoming hyperedges and all the vertices of B have incoming hyperedges and no outgoing hyperedges, then the hypergraph is Ricci flat . Also If the set of vertices can be divided into 3 sets, A, B, C such that all the vertices in these sets are connected to the vertices of the other sets as indicated in the right diagram, then the hypergraph is Ricci flat.*
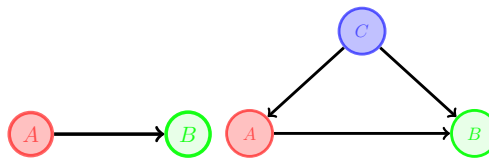

Figure 5.12

Proof. Based on the construction, for the two set partitioning, for every hyperedge, the masses are in the source set (A) which is at distance one from the holes which are in the sink set (B). So μ_1 is equal to 1 and the hypergraph is Ricci flat . For the other case, since we are assuming that all the vertices of A are connected to all the vertices of B and similarly for other connections the same condition holds, for every hyperedge $e : A \to B$, the distance between any incoming neighbour of A to any outgoing neighbour of B is one. So μ_1 is equal to 1 (and obviously by construction $\mu_0 = 0$). Therefore the hypergraph is Ricci flat .

□

Remark 5.2.26. *The convese of the previous theorem is not necessarily true. However, If in a Ricci flat directed hypergraph for every directed hyperedge e there is no incoming hyperedge to its tail set and there is no outgoing hyperedge from its head set, then the set of vertices in this directed hypergraph can be partitioned into two sets A and B as above. Since we put all the tail sets of all of directed hyperedges in set A and all the head sets of all of directed hyperedges in set B*

In the above theorem, for 3-set partitioning, in contrast to the 2-set partitioning, the sets are partitioned into source, saddle and sink sets. The vertices in a saddle have both incoming and outgoing hyperedges. Also similar to the Ricci 1 case, connections inside any of these 3 sets might violate constant curvature along different hyperedges. As the last case, in the following part we introduce a class of directed hypergraphs with the most negative curvature.

Remark 5.2.27. *Examples of Ricci flat directed hypergraphs can be constructed in which the set of their vertices is partitioned into 3 sets, but not all the above connections are present. In these hypergraphs, as before the presence of internal hyperedges (Likewise, connections inside each of these sets) might violate the flatnesses as can be seen in the next figure.*
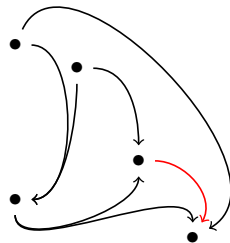

Figure 5.13

- **Ricci negative (-2) directed hypergraphs**

Proposition 5.2.28. *If the set of vertices of a directed hypergraph can be divided into 4 sets, A ,B , C and D such that all the vertices in these sets are connected to the vertices of the other sets as indicated, then the hypergraph is Ricci -2 . The presence of internal hyperedges (connections inside each of these sets) might violate constant curvature along different hyperedges.*
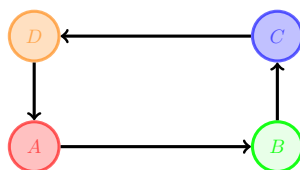

Figure 5.14

Proof. Here for every hyperedge $e : A \to B$, the distance between any incoming neighbour of A to any outgoing neighbour of B is 3. Therefore all $\mu_i = 0$, except $\mu_3 = 1$, and every hyperedge has curvature -2. $\qquad\square$

Remark 5.2.29. *Although we have presented some general examples of directed Ricci flat and -2 hypergraphs, we still cannot classify them. Also playing with (5.2) and considering different values of the $\mu_i s$, we can obtain non-negative, negative and non-positive curvatures for hyperedges, and possibly some Ricci constant hypergraphs.*

We can extend our constructions to weighted directed hypergraphs where the vertices and hyperedges may both carry weights. The vertices may carry different weights depending on the hyperedges they are involved in (This can be represented by a vector of the dimension of the hyperedge set with non-negative components. Here, zero means the corresponding hyperedge does not involve that vertex). For a specified hyperedge whose curvature we want to measure, the weights of its vertices need to be fixed, of course. In this case we denote the vertex and hyperedge weights by w_v and w_e respectively.

Definition 5.2.30.
$$\kappa(e) := 1 - W(\mu_{A^{in}}, \mu_{B^{out}})$$

where the probability measures $\mu_{A^{in}}$ (called mass) and $\mu_{B^{out}}$ (called hole), are defined on V as follows: Let $H = (V, E)$ be a weighed directed hypergraph and $e \in E$ an arbitrary directed hyperedge such that $A = \{x_1, \ldots, x_n\} \xrightarrow{e} B = \{y_1, \ldots, y_m\}$ $(n, m \leq |V|)$. We define the Ricci curvature of this hyperedge as

$$\kappa(e) := 1 - W(\mu_{A^{in}}, \mu_{B^{out}})$$

where the probability measures $\mu_{A^{in}}$ and $\mu_{B^{out}}$ are defined on V as follows:

$\mu_{A^{in}} = \sum_{i=1}^{n} \mu_{x_i}^{in} quad \forall 1 \leq i \leq n \quad$ *and* $\forall z \in V(H)$
and $\mu_{x_i}^{in}(z)$ *is :*

$$\begin{cases} 0 & z = x_i \quad \& \quad d_{x_i}^{in} \neq 0 \\ \frac{w_{x_i}}{\sum_{i=1}^{n} w_{x_i}} & z = x_i \quad \& \quad d_{x_i}^{in} = 0 \\ \sum_{e';z \in A_{e'}, \, x_i \in B_{e'}} \frac{w_{x_i}}{\sum_{x_j \in A} w_{x_j}} \times \frac{w_{e'}}{\sum_e w_{e:z \to A}} \times \frac{w_z}{\sum_{z \in A_{e'}} w_z} & z \neq x_i \quad \& \quad z \in A_{e'} \\ 0 & otherwise \end{cases}$$

Similarly,

$\mu_{B^{out}} = \sum_{j=1}^{m} \mu_{y_j}^{out}$ *where* $\forall 1 \leq j \leq m, z \in V(H)$:
where $\mu_{y_j}^{out}(z)$ *is:*

$$\begin{cases} 0 & z = y_j \quad \& \quad d^{out}_{y_j} \neq 0 \\[2mm] \frac{w_{y_j}}{\sum_{y_i \in B} w_{y_i}} & z = y_j \quad \& \quad d^{out}_{y_j} = 0 \\[2mm] \sum_{e';\, y_j \in A_{e'},\, z \in B_{e'}} \frac{w_{y_j}}{\sum_{y_i \in B} w_{y_i}} \times \frac{w_{e'}}{\sum_e w_{e:B \to z}} \times \frac{w_z}{\sum_{z \in B_{e'}} w_z} & z \neq y_j \quad \& \quad z \in B_{e'} \\[2mm] 0 & otherwise \end{cases}$$

Remark 5.2.31. *In weighted directed graphs, the Proposition 5.2.21 does not hold because, due to the weights we might have masses which coincide with holes of different sizes and therefore it violates Ricci 1 condition. For instance if we consider two directed 3-cycles which have one edge in common, by considering non-equal weights assigned to two other edges in the two cycles, the curvature of the common edge is not one although we have a 3 set partitioning in which all the required connections exist.*

Further differences between directed and undirected (hyper)graphs

- **In directed (hyper)graphs, lower curvature bounds no longer control random walks.**

  Also since the Wasserstein distance no longer needs to satisfy a triangle inequality, we cannot define curvatures for vertex sets that are not connected by a hyperedge. These problems come essentially from the fact that we consider incoming edges at the tail A and outgoing edges at the head B of a hyperedge. In principle, we could of course also consider in-in or out-out relationships instead, but then, we might not always be able to move our masses, and so, curvatures might then become $-\infty$. This can only be avoided if we assume some strong connectedness condition in the directed case (see for instance [57]). Such a condition, however, is typically not satisfied in empirical data sets.

- **The curvature of a directed (hyper)graph might be rather different from that of the underlying undirected (hyper)graph.**

  For instance, in an undirected graph, every edge in a quadrangle has curvature zero. But a directed k-cycle where $k \geq 4$ is negatively curved.

- **Directed Triangles**

  In undirected graphs, it has been proven that the local clustering coefficient at each vertex can control the scalar curvature of any vertex which by definition is obtained by averaging over the Ricci curvature of all the edges connecting to that vertex (see Corollary 1 in [33]). In the undirected graph case, the local clustering coefficient is based on the number of triangles containing that vertex and its neighbours. In the directed case, after fixing the direction of every hyperedge, we encounter with 4 different types of triangles which share the property of having a directed edge that goes out from A and enters into the set B. Therefore in contrast to the undirected

graph case, not all directed triangles but only some of them affect the curvature; in fact, for μ_0 the presence of directed 3-cycles containing the vertices of A and B and of vertices u where $u \to x_i \to y_j \to u, u \in A^{in}(u \to A)$ and $u \in B^{out}(B \to u)$ increases the curvature of the corresponding hyperedge since they directly increase the amount of μ_0.

In contrast, those directed triangles which contain vertices of A and B and u in such a way that $x_i \to u, x_i \to y_j \to u, u \in A^{out}(A \to u)$ and $u \in B^{out}(B \to u)$ and those containing A and B and u such that $u \to x_i \to y_j, u \to y_j, u \in A^{in}(u \to A), u \in B^{in}(u \to B)$ might affect on the amount of μ_2 and thereby can make the curvature less negative. The last type of directed triangles are those which include vertices of A and B, outgoing vertices of A and incoming vertices to the set B, but they do not affect any of the μ_is and therefore the curvature. For instance in the following directed graph, for computing the curvature of the green edge, the triangle consisting of the red and green edges affects μ_0. Both triangles including orange-green and blue-green edges have an effect on μ_2 and the curvature is not affected by the presence of the triangle of the pink-green edges.
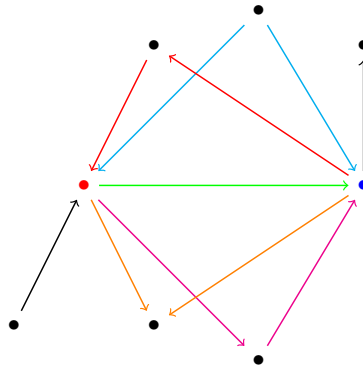

Figure 5.15

6

Networks can be curved!

As already mentioned, in traditional analysis of complex networks, we were modelling complex networks by (di)graphs and were using vertex based measures to determine the structure (local and global) of these networks, measures such as node degree and (local) clustering coefficient. However, in the modern analysis, we take higher order interactions into account based on modelling via (di)hypergraphs and simplicial complexes and we are trying to develop (hyper)edge (or simplex) based measures with the help of ideas originated from Rimannian smooth settings for probing local or global structures. This paradigm is obviously fundamental for the analysis of empirical networks, be they from the biological sciences or other domains. In this last chapter we show that Ricci curvature and in particular what we developed in previous chapter can be used as a very powerful tool to capture some important structures in variety of complex networks.

6.1 Preliminaries

In recent years, alongside Ollivier Ricci curvature, another type of Ricci curvature, originaly defiend by Forman in 2003, has been used for analysing complex network modelled as directed and undirected graphs. Forman defined his notion of Ricci curvature for cell complexes based on totally different ideas coming from Riemannian Geometry[26]. While Forman's definition applies to general CW-complexes, here we recall it for simplicial complexes. Forman defines functions :

$$F_p : \{p - \text{simplices}\} \longrightarrow \mathbb{R}$$

by putting, for a p-simplex α,

$$
\begin{aligned}
F_p(\alpha) \quad := \quad & \sharp\{(p+1)\text{-simplices } \beta > \alpha\} + \sharp\{(p-1)\text{-simplices } \gamma < \alpha\} \\
& - \quad \sharp\{\text{parallel neighbors of } \alpha\},
\end{aligned}
$$

where $\beta > \alpha$ means that the p-simplex α is contained in the boundary of the $(p+1)$-simplex β, and analogously, $\gamma < \alpha$ means that the $(p-1)$-simplex γ is contained in the boundary of α; a parallel neighbour of the p-simplex α is another simplex α' of the same dimension that is disjoint from α, but either contained in the boundary of some $(p+1)$-simplex that also contains α in its boundary or contain some $(p-1)$-simplex in its boundary that is also contained in the boundary of α, but not both.

Recently, Leal et.al generalised this notion to both undirected and directed hypergraphs [38]. Here we recall this definition for the special case of directed hypergraphs which currently are vastly used for modelling many biochemical networks. Consider we have a directed hypergraph, denoted by a couple $H = (V, E)$ that V is a set of vertices and E a set of ordered pairs of subsets of V called hyperedges. Given a hyperedge $e : A = \{x_1, \ldots, x_n\} \to B = \{y_1, \ldots, y_m\}$ in E, where A and B are two non-empty subsets of V, respectively called the tail and the head of e, Forman-Ricci curvature of e is defined as follows:

$$F(e) := |A| + |B| - \sum_{x_i \in A} \text{in-deg}(x_i) - \sum_{y_j \in B} \text{out-deg}(y_j) \tag{6.1}$$

where the in(out)-degree of a vertex $x_i(y_j)$ is the number of hyperedges that have $x_i(y_j)$ as part of its head (tail).

In fact, in [38], different types of Forman Ricci curvature of a directed hyperedge have been introduced. Here we use only the version in (6.1) to be able to compare it with the other notion of Ricci curvature, namely Ollivier, for a given hyperedge.

6.2 Why Ricci curvature?

In the past few years, both Ollivier-Ricci and Forman-Ricci curvatures have been extensively used for analysing variety of structures and networks. For the case of graphs it has been shown that these curvature notions shed light on different aspects of network structure and behaviour. Moreover applying these tools to a wide range of both model and real-world graph-networks already shows that the two discretizations of Ricci curvature are highly correlated in many networks that are modelled as graphs [50]. More importantly, to name a few, the two curvature notions have been used for differentiating cancer networks [51], characterizing the structure of financial systems [49] and even to infer COVID-19 epidemic network fragility and systemic risk [11]. Here we extend the utility of these two popular notions of Ricci curvature, introduced in previous section (and in [13]) by us and in [38] by Leal et.al, to the more general and complex case of directed hypergraphs and in particular

real hypernetworks. Specifically we show Ollivier-Ricci curvature notion that we developed, is a powerful tool for analysing local structures of complex networks which are faithfully modelled as directed hypergraphs, networks such as chemical reactions.

- **Forman and Ollivier Ricci curvatures are complementary tools for the local identification and analysis of connectivity motif and patterns.**
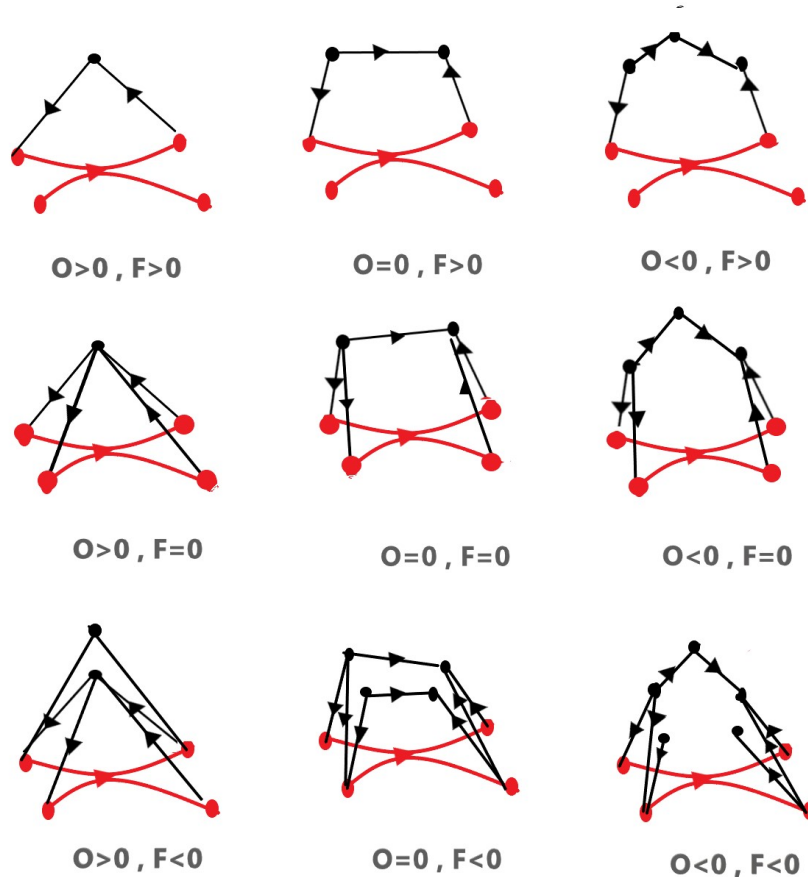

Figure 6.1

We discuss signs and values of F and O for the red hyperedges of the nine directed hypergraphs presented in the above diagram, based on the connections of their tails and heads; when we go from left to right, as we are changing some of the shortcrust for moving masses to holes, Ollivier-Ricci curvature is decreasing and specifically its sign changes while the sign of F is fixed. As we see in the left column, triangles are present as the best type of short-cuts (where some masses and holes coincide) and in the middle column we have quadrangles which are substituted with pentagons in the right columns where distances between each mass and each hole of e is two. On the other hand, when we move vertically in the plot, the F sign changes as we increase the number of incoming hyperedges to the set A and outgoing hyperedges from the set B while the sign of O is fixed. In the diagonal, directed hyperedges have the same sign for both curvatures.

- **Geometry of Hyperloops.**

  As already defined, a directed hyperloop in a directed hypergraph is a directed hyper-edge e in which its tail A and head B have non-empty intersection.
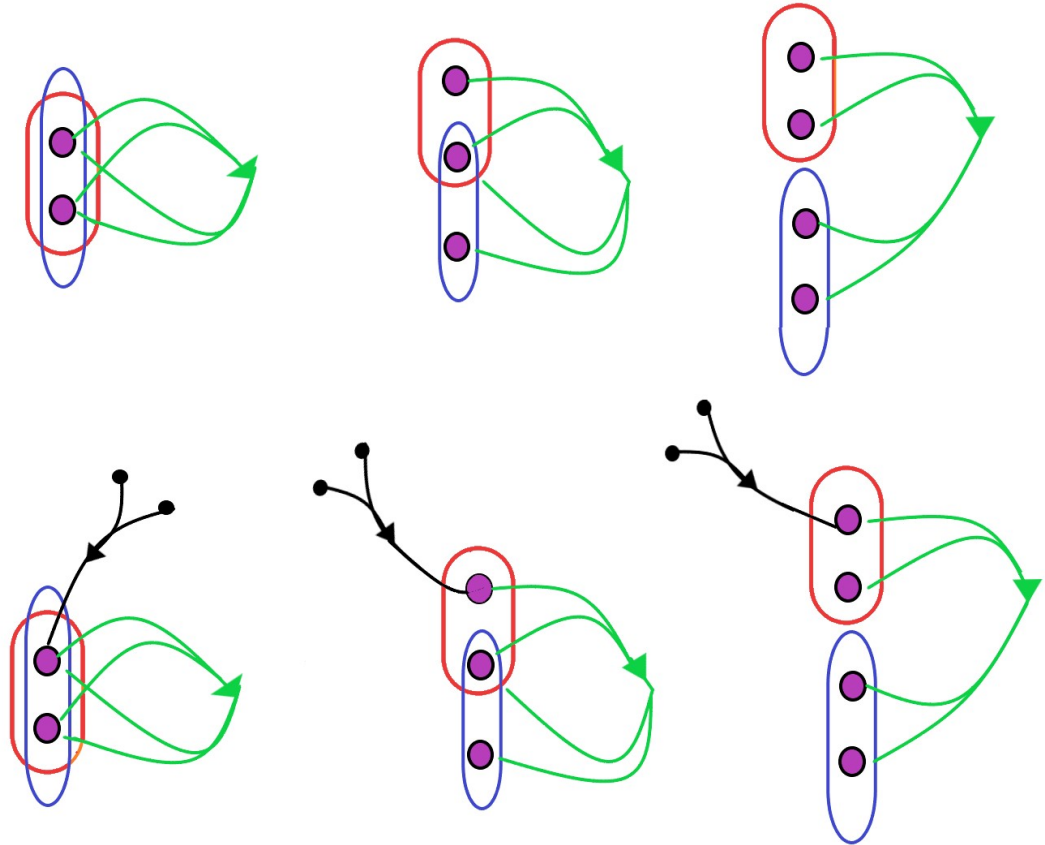

Figure 6.2

In the above figure, we are concerning about Forman-Ricci and Ollivier-Ricci curvatures of the green hyperedges and their tail and head are respectively represented by red and blue ellipse.

Base on our definition, the green hyperedges in the left and middle columns are hyperloops while in the right columns we have no hyperloops.

When in a hyperedge e, the A and B coincide and furthermore the hypereloop is isolated, as shown in the top left hyperloop, $F(e) = 0$ while $O(e) = 1$. If the hyperedge is not isolated, both curvature notions might change. If we move down in columns, we see that both $F(e)$ and $O(e)$ decrease, as the result of the incoming neighbours added to the tail of e. On the other side when we move from left to right horizontally in each row, Forman-Ricci curvature of the green hyperedges increases while Ollivier-Ricci curvature decreases.

For instance in the first row the amount of Ollivier-Ricci curvatures are 1, $1/2$ and 0

respectively from left to right while Forman-Ricci curvatures are respectively 0, 2 and 4.

- **Detecting local/global important structures such as clustering, sparsity, bottleneck or redundant reactions.**

  One of the best examples of complex networks that can be modelled by directed hypergraphs are metabolic networks. Each chemical reaction can be represented faithfully by a directed hyperedge $e : A \to B$, where A and B are respectively the set of educts and the set of products of the reaction. Here, we use our geometric tool, Ollivier Ricci curvature, to investigate the structure of the directed hypergraph that represents the *E. coli* metabolic hypernetwork. In particular, we present the curvature distribution fingerprints of Ollivier-Ricci curvature for this network.The metabolism of this bacterium, reported in [48] (K-12 (iJR904GSM/GPR)), is modelled as a directed hypergraph where vertices represent chemical substances (metabolites) and hyperedges represent metabolic reactions. There are 625 vertices (metabolites, $|V| = 625$) and 1176 hyperedges (chemical reactions, $|E| = 1,176$). It has been observed that in the metabolic network of *E. coli*, (and in general in the whole Chemical Space [40]), 90% of chemical reactions have at most three reactants and three products. On the other hand when considering the number of incoming neighbours of reactants and outgoing neighbours of products for every reaction, frequencies are of the order of hundreds and, for some reactions, almost the whole set of metabolites, as shown in the following diagram.
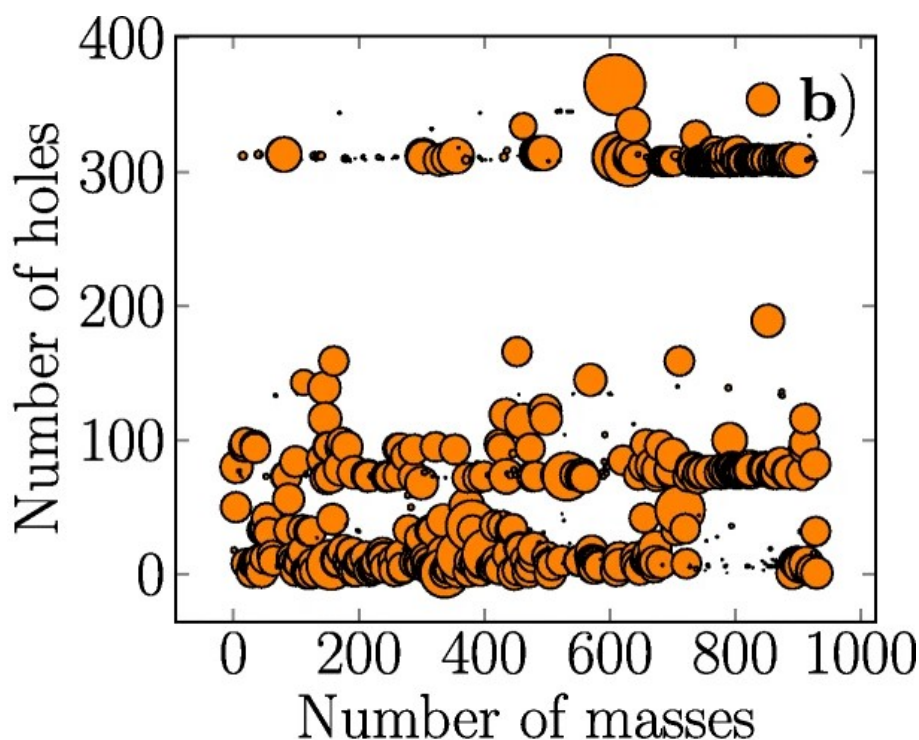

Figure 6.3

In networks that are modelled by undirected graphs, one very main task is to quantify the amount of clustering around a vertex. There we use measures such as local clustering coefficient to determine the density of triangles including each vertex. As mentioned before, local clustering coefficient of a vertex in an undirected graph is directly related to the scalar curvature at a vertex where the scalar curvature is obtained by taking the average of Ollivier Ricci curvatures of the edges including that vertex. However, when it comes to directed structures and edge-based measures, determining the amount of overlap between adjacent neighbourhoods becomes important. The question that arises is that how close the neighbourhoods of sets A and B are in such structures? As we saw, Ollivier Ricci curvature is one main tool for quantifying closeness of neighbourhoods and in particular in real networks such as metabolic reactions we are interested in measuring closeness based on the distance between masses and holes of a reaction. The Ollivier-Ricci curvature distribution in the next plot shows that in the metabolic network of *E. coli* most masses and holes are at distance less than 3, since the vast majority have curvature greater than -0.5. Also less than 10% of incoming and outgoing neighbours are at distance 3. Only four reactions have curvature -2, which shows that their masses are at distance three from their holes.
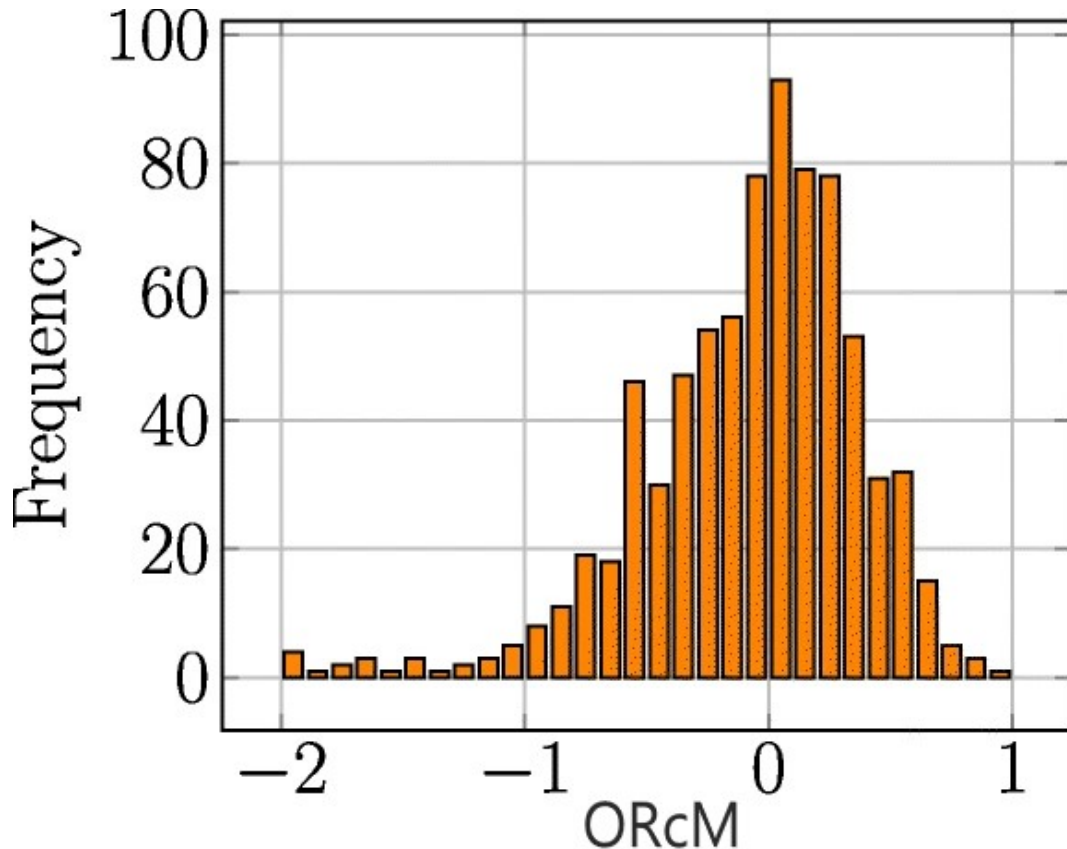

Figure 6.4

- **Shuffling of metabolic network of *E.coli* can be nicely detected by both Ollivier and Forman Ricci curvatures.**
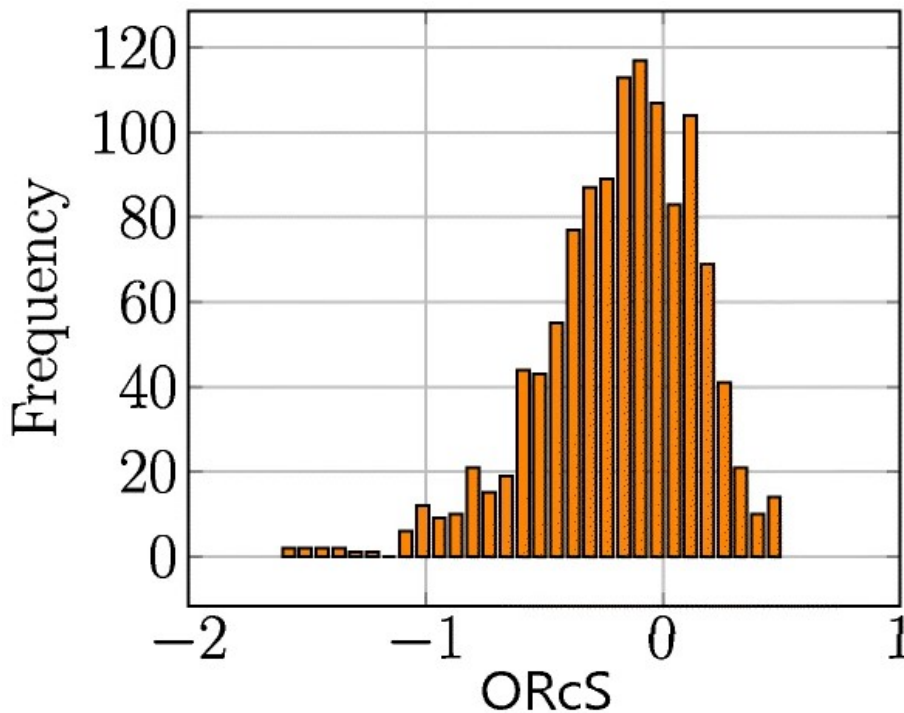
Another very usual framework in analysing complex networks is to compare them with the randomly generated models. Specifically we can shuffle hyperedges of a directed hypergraph. As in the shuffling process degree sequence and size of hyperedges are stable, the shuffled network is very close to the original case and therefore its very desirable to look for measures or tools that can detect the shuffling process; in the shuffling experiment, we start with the metabolic network M and end up with a directed hypergraph S of the same size (distributions of tail and head sizes are fixed) and with the same degree sequence. As we see in the above figure, the distributions of shuffled metabolic network clearly deviates from the original network of metabolic of *E.coli* and thus this confirms that our notion of curvature detect differences that the degree sequence and size of hyperdges can not. Also as presented in [37], the same principle works when we consider distribution of Forman-Ricci curvature for both metabolic network of *E.coli* as well as its corresponding shuffled network.

Remark 6.2.1. *In [37], we introduce a random model of directed hypergraphs, a hypergraph version of the Erdös-Rényi (ER) model, and explore the distribution of both Forman and Ollivier Ricci curvatures. There, we have shown that the distributions of both Forman and Ollivier Ricci curvatures for E.coli are very different from those of random hypergraphs. Also as its shown in [38], frequent values of Forman-Ricci curvatures help us to distinguish bottle neck and redundant reactions in the metabolic network.*

Remark 6.2.2. *In [12], we have summarized the relation-based measures, Ollivier [13].*

and Forman [38] Ricci curvatures , both for (di) graphs, that being the simplest case, and for (directed) hypergraphs; Specifically, we have analysed the distribution of the two types of Ricci-curvatures [13, 38] for binary protein interaction networks in human and fission yeast which are modelled as undirected graph; we see that the distribution of curvature values can point us to biologically relevant properties of the interaction statistics in the PPI networks of different species. To illustrate an application to directed networks, we have studied the transcriptional regulatory network (TRN) of an important human pathogen. Lastly as a network modelled as directed hypergraph, we have studied another metabolic network, metabolic network of Mycobacterium tuberculosis H37Rv; in particular, we see that combination of the two geometric measures that have been mentioned, can reveal the fundamental structural properties of specific reactions inside the metabolic network. Both evaluating the statistical distributions of these quantities and comparing them for different networks, and analysing those reactions that produce particularly prominent values for them in more detail should yield deeper insight into the structure of metabolic networks.

Bibliography

[1] Shahab Asoodeh, Tingran Gao, and James Evans. Curvature of hypergraphs via multi-marginal optimal transport. In *2018 IEEE Conference on Decision and Control (CDC)*, pages 1180–1185. IEEE, 2018.

[2] Anirban Banerjee. On the spectrum of hypergraphs, 2017.

[3] A. Banyaga and D.Hurtubise. *Lectures on Morse homology*. Kluwer, 2004.

[4] Augustin Banyaga and David E. Hurtubise. Morse-Bott homology. *Transactions of the American Mathematical Society*, 362(8):3997–4043, 2010.

[5] Frank Bauer. Normalized graph laplacians for directed graphs, 2012.

[6] Bruno Benedetti. Discrete Morse theory is at least as perfect as Morse theory. *arXiv e-prints*, page arXiv:1010.0548, October 2010.

[7] Raoul Bott. Morse theory indomitable. *Publications Mathématiques de l'IHÉS*, 68:99–114, 1988.

[8] Fan Chung. Laplacians and the cheeger inequality for directed graphs. *Annals of Combinatorics*, 9:1–19, 04 2005.

[9] C. Conley. *Isolated invariant sets and the Morse index*. CBMS Reg. Conf. Ser. Math. 38, AMS, Providence, R.I., 1978.

[10] C. Conley and E. Zehnder. Morse-type index theory for flows and periodic solutions for Hamiltonian equations. *Comm. Pure Appl. Math.*, 37:207–253, 1984.

[11] Danillo Barros de Souza, Fernando A. N. Santos, Everlon Figuerôa dos Santos, Jailson B. Correia, Hernande P. da Silva, José Luiz de Lima Filho, and Jones Albuquerque. Using curvature to infer covid-19 fractal epidemic network fragility and systemic risk. *medRxiv*, 2020.

[12] Marzieh Eidi, Amirhossein Farzam, Wilmer Leal, Areejit Samal, and Jürgen Jost. Edge-based analysis of networks: curvatures of graphs and hypergraphs. *Theory in Biosciences*, 139(4):337–348, Nov 2020.

[13] Marzieh Eidi and Jürgen Jost. Ollivier ricci curvature of directed hypergraphs. *Scientific Reports*, 10(1):12466, 2020.

[14] Marzieh Eidi and Jürgen Jost. Floer homology: From generalized morse-smale dynamical systems to forman's combinatorial vector fields, 2021.

[15] E. Estrada. *The Structure of Complex Networks*. Oxford Univ. Press, 2012.

[16] C. Joslyn et al. Hypernetwork science: From multidimensional networks to computational topology. Technical report, arXiv:2003.11782v1, 2020.

[17] A. Floer. An instanton invariant for 3-manifolds. *Comm.Math.Phys.*, 118:215–240, 1988.

[18] A. Floer. Morse theory for Lagrangian intersections. *J.Diff.Geom.*, 28:513–547, 1988.

[19] A. Floer. A relative Morse index for the symplectic action. *Comm.Pure Appl.Math.*, 41:393–407, 1988.

[20] A. Floer. Witten's complex and infinite dimensional Morse theory. *J. Diff. Geom.*, 30:207–221, 1989.

[21] A. Floer and H. Hofer. Coherent orientations for periodic orbit problems in symplectic geometry. *Math. Z.*, 212:13–38, 1993.

[22] Andreas Floer. The unregularized gradient flow of the symplectic action. *Communications on Pure and Applied Mathematics*, 41(6):775–813, 1988.

[23] R. Forman. Combinatorial vector fields and dynamical systems. *Mathematische Zeitschrift*, 228:629–681, 1998.

[24] R. Forman. Witten-Morse theory for cell complexes. *Topology*, 37:945–979, 1998.

[25] Robin Forman. Morse theory for cell complexes. *Advances in Mathematics*, 134(1):90–145, 1998.

[26] Robin Forman. Bochner's method for cell complexes and combinatorial ricci curvature. *Discrete & Computational Geometry*, 29:323–374, 2003.

[27] John M. Franks. *Homology and Dynamical Systems*. American Mathematical Society, 1982.

[28] Arne Holst. Volume of data/information.

[29] David E. Hurtubise. Three approaches to Morse-Bott homology, 2013.

[30] M. Jackson. *Social and economic networks*. Princeton Univ. Press, 2008.

[31] J. Jost. *Dynamical Systems*. Springer-Verlag Berlin Heidelberg, 2005.

[32] J. Jost. *Riemannian geometry and geometric analysis*. Springer, 7th ed., 2017.

[33] Jürgen Jost and Shiping Liu. Ollivier's Ricci curvature, local clustering and curvature-dimension inequalities on graphs. *Discrete & Computational Geometry*, 51(2):300–322, 2014.

[34] Kevin P Knudson. *Morse theory*. WORLD SCIENTIFIC, 2015.

[35] Elena Di Lavore, Wilmer Leal, and Valeria de Paiva. Dialectica petri nets, 2021.

[36] Wilmer Leal, Marzieh Eidi, and Jürgen Jost. Curvature-based analysis of directed hypernetworks. In Hocine Cherifi, editor, *Complex networks 2019 : the 8th international conference on complex networks and their applications ; December 10 - 12, 2019 Lisbon, Portugal ; book of abstract*, pages 32–34. International Conference on Complex Networks & Their Applications, [s.l.], 2019.

[37] Wilmer Leal, Marzieh Eidi, and Jürgen Jost. Ricci curvature of random and empirical directed hypernetworks. *Applied network science*, 5:65, 2020.

[38] Wilmer Leal, Guillermo Restrepo, Peter F. Stadler, and Jürgen Jost. Forman-ricci curvature for hypergraphs. *arXiv*, page 1811.07825, 2018.

[39] Yong Lin, Linyuan Lu, and Shing-Tung Yau. Ricci curvature of graphs. *Tohoku Mathematical Journal*, 63(4):605 – 627, 2011.

[40] Eugenio J. Llanos, Wilmer Leal, Duc H. Luu, Jürgen Jost, Peter F. Stadler, and Guillermo Restrepo. Exploration of the chemical space and its three historical regimes. *Proceedings of the National Academy of Sciences*, 116(26):12660–12665, 2019.

[41] J. Lohkamp. Negatively Ricci curved manifolds. *Bull. AMS*, 27:288–292, 1992.

[42] K. R. Meyer. Energy functions for Morse Smale systems. *American Journal of Mathematics*, 90(4):1031–1040, 1968.

[43] Marston Morse. Relations between the critical points of a real function of n independent variables. *Transactions of the American Mathematical Society*, 27(3):345–396, 1925.

[44] M. Newman, A. Barabási, and D. J. Watts. *The Structure and Dynamics of Networks*. Princeton University Press, 2006.

[45] Yann Ollivier. Ricci curvature of Markov chains on metric spaces. *Journal of Functional Analysis*, 256(3):810–864, February 2009.

[46] Yann Ollivier. A visual introduction to Riemannian curvatures and some discrete generalizations. *Analysis and Geometry of Metric Measure Spaces: Lecture Notes of the 50th Séminaire de Mathématiques Supérieures (SMS), Montréal*, 56:197–219, 2011.

[47] Ryunosuke Ozawa, Yohei Sakurai, and Taiki Yamada. Geometric and spectral properties of directed graphs under a lower ricci curvature bound, 2020.

[48] Jennifer L. Reed, Thuy D. Vo, Christophe H. Schilling, and Bernhard Ø. Palsson. An expanded genome-scale model of escherichia coli k-12 (ijr904 gsm/gpr). *Genome Biol.*, 4:R54.1–R54.12, 2003.

[49] Areejit Samal, Hirdesh K. Pharasi, Sarath Jyotsna Ramaia, Harish Kannan, Emil Saucan, JÃŒrgen Jost, and Anirban Chakraborti. Network geometry and market instability. *Royal Society Open Science*, 8(2):201734, 2021.

[50] Areejit Samal, RP Sreejith, Jiao Gu, Shiping Liu, Emil Saucan, and Jürgen Jost. Comparative analysis of two discretizations of Ricci curvature for complex networks. *Scientific reports*, 8, 2018.

[51] Romeil Sandhu, Tryphon Georgiou, Ed Reznik, Liangjia Zhu, Ivan Kolesov, Yasin Senbabaoglu, and Allen Tannenbaum. Graph curvature for differentiating cancer networks. *Sci Rep*, 5:12323, 2015 Jul 14 2015.

[52] M. Schwarz. *Morse homology*. Birkhäuser, 1993.

[53] Nicholas A. Scoville. *Discrete Morse Theory*. American Mathematical Society, 2019.

[54] Stephen Smale. Morse inequalities for a dynamical system. *Bulletin of the American Mathematical Society*, 66(1):43 – 49, 1960.

[55] Stephen Smale. On gradient dynamical systems. *Annals of Mathematics*, 74(1):199–206, 1961.

[56] J. Smoller. *Shock waves and reaction-diffusion equations*. Springer, 2nd ed., 1994.

[57] Taiki Yamada. The Ricci curvature on directed graphs. *arXiv preprint arXiv:1602.07779*, 2016.